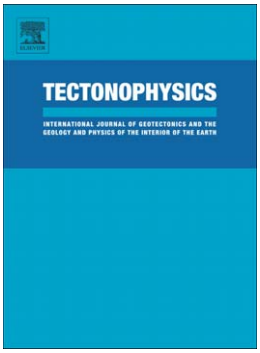

Restoring paleomagnetic data in complex superposed folding settings: the Boltaña anticline (Southern Pyrenees)

T. Mochales, E.L. Pueyo, A.M. Casas, A. Barnolas

PII: S0040-1951(16)00045-7
DOI: doi: 10.1016/j.tecto.2016.01.008
Reference: TECTO 126902

To appear in: *Tectonophysics*

Received date: 12 January 2015
Revised date: 30 December 2015
Accepted date: 4 January 2016

Please cite this article as: Mochales, T., Pueyo, E.L., Casas, A.M., Barnolas, A., Restoring paleomagnetic data in complex superposed folding settings: the Boltaña anticline (Southern Pyrenees), *Tectonophysics* (2016), doi: 10.1016/j.tecto.2016.01.008

Restoring paleomagnetic data in complex superposed folding settings: the Boltaña anticline (Southern Pyrenees)

T. Mochales [1, 2)(*]; E.L. Pueyo [2]; A.M. Casas [3]; A. Barnolas [1]

[1] Instituto Geológico y Minero de España, c/ Rios Rosas 23, 28003 Madrid (Spain). taniamochales@gmail.com, tonibarnolas@hotmail.com

[2] Instituto Geologico y Minero de España. Unidad de Zaragoza. c/ Manuel Lasala 44, 50006 Zaragoza (Spain). unaim@igme.es

[3] Departamento de Ciencias de la Tierra, Universidad de Zaragoza. c/ Pedro Cerbuna 12, 50009 Zaragoza (Spain). acasas@unizar.es

ABSTRACT

Complex kinematic scenarios in fold-and-thrust belts often produce superposed and non-coaxial folding. Interpretation of primary linear indicators must be based on a careful restoration to the undeformed stage following the reverse order of the deformation events. Therefore, sequential restoration to the ancient coordinate system is of key importance to obtain reliable kinematic interpretations using paleomagnetic data. In this paper, a new paleomagnetic study in the western flank of the Boltaña anticline (Southern Pyrenees) illustrates a case study of a complex tectonic setting having superposed, non-coaxial folds. The first stage of NW-SE folding linked to the oblique Boltaña anticline took place during Lutetian times. The second stage was linked to the vertical axis rotation and placed the Boltaña anticline in its present-day N-S

configuration. Our data support a long-lasting Lutetian to Priabonian period with main rotational activity during the Bartonian-Priabonian; other authors support a coeval VAR coeval with anticlinal growth. The third stage resulted in southwards tilting related to the emplacement of the N120E striking Guarga basement thrust (Oligocene-Early Miocene). Based on this deformational history, a sequential restoration was applied and compared with the classic bedding correction. At the site scale, single bedding correction gives errors ranging between 31° to -31° in the estimation of vertical axis rotations. At the locality scale, in sites grouped in three folds (from W to E Arbella, Planillo and San Felizes), the bedding corrected data display rotation values in accordance to those found in the Ainsa Basin by other authors. Sequential restoration (based on the afore-mentioned evolution in three-steps) improves both some locality-means and the internal consistency of the data. Therefore, reasonably-constrained sequential restoration becomes essential to reconstruct the actual history of superposed folding areas.

Keywords: Paleomagnetism, vertical axis rotation, restoration, sequential, superimposed folding, Pyrenees.

1. INTRODUCTION

Paleomagnetism is an excellent technique to decipher kinematics of folding and thrusting due to the possibility of quantifying vertical axis rotations (VAR). It is one of the very few tools that allow completing the three-dimensional understanding of fold and thrust belts, all together with surface and subsurface data and structural analysis, since it constrains the deformed and undeformed stages (McCaig & McClelland, 1992; Allerton, 1998; Waldhör and Appel, 2009; Sussman et al., 2012; Ramón et al., 2012;

Pueyo et al., 2015). Conversely, other kinematic indicators of strain and stress are not necessarily related to the pre-deformational stage or cannot be accurately dated with respect to folding.

Paleomagnetic data, both local sites and references, have to accomplish several reliability criteria based on laboratory, processing and statistical procedures as well as geological and geomagnetic constraints (Van der Voo, 1990). Apart from other potential error sources, such as internal deformation (Lowrie et al., 1986; Van der Pluijm, 1987; Kodama, 1988; Borradaile, 1997), inclination shallowing observed during compaction (Kodama, 1997) or overlapping with younger components (Rodríguez-Pintó et al., 2011 and 2013a), simple restoration (bedding correction) of paleomagnetic vectors from the geographic coordinate reference system (in situ) to the paleogeographic one, is a potential source of large errors (Pueyo, 2000 and 2010). This paper focuses on the problem of paleomagnetic restoration where superposed folding occurs. During the past years, some papers have dealt with the restoration problem in non-cylindrical or complex structures, such as plunging folds (Zotkevich, 1972; Sellés, 1988; Stewart 1995), fold closures (Stewart and Jackson, 1995), conical folds (Pueyo et al., 2003a; Pastor-Galán et al., 2012) or thrust ramp geometries (Pueyo et al., 2003b). Nevertheless, superposed folding has received very little attention so far (Weil, 2006; Waldhör and Appel, 2009).

The oblique structures of the South Central Pyrenees (Fig. 1) have traditionally attracted the attention of the scientific community. Recently, numerous studies have focused on characterizing and understanding of vertical-axis rotations in the External Sierras and in the so-called Ainsa Oblique Zone (Dinarès-Turell et al., 1992; Parés and Dinarès, 1993; Pueyo, 2000; Pueyo et al., 2002; Fernández-Bellón, 2004; Mochales, 2011; Mochales et al., 2012a and 2012b; Rodriguez-Pintó et al., 2011; Oliva-Urcia et all., 2012;

Rodriguez-Pintó et al., 2013a; Beamud, 2013; Muñoz et al. 2013) where numerous N-S trending structures contrast with the main WNW- ESE Pyrenean direction; i.e. Pico del Aguila, Boltaña, Mediano, Balzes anticlines. In this paper, for the analysis of sequential vs. simple restoration in paleomagnetism, we introduce 13 new paleomagnetic sites from the Jánovas area, located in the western limb of the Boltaña anticline (northern sector), and we consider also 2 sites from previous studies in the region (Pueyo, 2000). In the Jánovas area, the Lutetian to Bartonian rocks of the frontal limb of the Boltaña anticline recorded three successive partially coeval and non-coaxial deformational episodes; folding, vertical axis rotation and oblique, passive tilting. Although there is not a total agreement on the timing and quantification of these deformational events, this controversial area is a perfect location to explore how the restoration method may affect the final interpretation of paleomagnetic data in complex scenarios. We will compare the sequential restoration following a reverse order of deformation events with the standard bedding correction to illustrate how large errors can be when polyphase deformation is not taken into account.

2. GEOLOGICAL SETTING

The Pyrenees represent the collision between the Iberian and European plates (Muñoz, 1992; Teixell, 1998; Rosenbaum et al., 2002) during Late Cretaceous to Miocene times. Two fold and thrust belts with opposite vergences were developed towards their respective foreland basins; Aquitaine to the North and Ebro to the South (Fig. 1). The South Pyrenean Zone comprises a set of allochthonous imbricated thrust sheets mostly developed in piggyback sequence (Séguret, 1972; Garrido-Megías, 1973; Cámara and Klimowitz, 1985; Muñoz, 1992). These thrust sheets are detached along Triassic

evaporites and incorporate Mesozoic and Cenozoic cover materials.

In the South Central sector, the South Pyrenean Central Unit (SPCU, Séguret, 1972) constitutes the main structural feature. From north to south the SPCU consists of three major thrust sheets (Fig. 1); 1) Cotiella-Bòixols where compressive deformation began during Late Cretaceous (Garrido-Megías, 1973; Simó, 1985; Bond and McClay, 1995; Muñoz et al., 1997; García-Senz, 2002; Martínez-Peña and Casas-Sainz, 2003; Mencos, 2010), 2) Montsec thrust sheet, active from Early to Late Ypresian times and was subsequently reactivated as an out-of-sequence thrust (after Garrido-Megías, 1973; Farrell et al., 1987; Vergés and Muñoz, 1990) or the coupled Peña Montañesa-Montsec system, active from the Paleocene to the Late Ypresian (Muñoz et al., 2013) and 3) the Sierras Marginales thrust sheet, active during Lutetian to Oligocene times (Garrido-Megías, 1973; Puigdefàbregas, 1975; Vergés and Muñoz, 1990; Millán, 1996; Teixell and Muñoz, 2000), which is responsible for the southernmost Pyrenean structure detached in the Triassic and the Eocene gypsum units (also forming the Barbastro anticline). Laterally westwards, the Sierras Marginales propagate into the External Sierras imbricate thrust sheet system, active from Late Eocene to Miocene times (Millán et al., 2000).

Distinct features of the South Pyrenean sole thrust in the central and western sectors are the slow westwards propagation of structures (Millán et al., 2000) and the regional gradient of shortening (Oliva-Urcia and Pueyo, 2007) that produce widespread regional vertical axis rotations. Because of these reasons, numerous structures transverse to the Pyrenean trend (WNW-ESE) were formed West of the SPCU in the External Sierras and in the Ainsa Oblique Zone, i.e. Mediano, Boltaña, Balzes, Pico del Águila anticlines (Puigdefàbregas, 1975; Poblet and Hardy, 1995; Millán et al., 2000; Poblet et al., 1998; Anastasio and Holl, 2001; Soto and Casas, 2001; Soto et al., 2002; Fernández-Bellón et

al., 2004; Vidal-Royo et al., 2011 and 2013; Muñoz et al., 2013; Rodríguez-Pintó et al., 2015). These N-S structures are progressively younger and smaller towards the W (Puigdefàbregas, 1975; Cámara and Klimowitz, 1985; Millán, 1996; Pueyo, 2000). Numerous paleomagnetic evidences indicate significant clockwise rotations (30-55°) related to the formation of the N-S structures (Parés and Dinarès, 1993; Pueyo et al., 2002; Fernández-Bellón 2004; Mochales et al., 2012a, b; Beamud, 2013; Muñoz et al., 2013).

The study here presented is focused on a series of minor folds linked to the western limb of the Boltaña anticline, a west-verging fault-propagation fold, related to two blind thrusts (Holl and Anastasio, 1995a a, b; Millán, 1996; Soto and Casas, 2001; Fernández-Bellón, 2004; Fernández-Bellón, et al., 2012; Tavani et al., 2006; Muñoz et al., 2013). We deal with the geometrical problems in the Jánovas area (NW sector of the anticline), where the existence of superposition of structural stages and the existence of growth strata compel to a special treatment for paleomagnetic data and serves as an example of data processing in complex structural settings.

2.1. The Jánovas sector

The studied area is located in the northern sector of the western limb of the Boltaña anticline (Ara river gorge, Fig. 2). The older outcropping rocks of the Boltaña anticline (in the pre-folding sequence) correspond to shallow marine limestones and siliciclastic sediments of Ypresian age, including five lithostratigraphic units: Alveoline limestones, Millaris, Metils, Yeba and Boltaña Fms. (more details in Van Lunsen, 1970; Ríos Aragüés et al., 1982, Barnolas et al., 1991; Fernández-Bellón, 2004; Mochales et al., 2012a). The age of this succession is well established by biostratigraphic (macroforaminifera) and magneostratigraphic studies (Mochales et al, 2012a). To the

North, the Boltaña Fm. ends with a slope erosional truncation buried by the onlap of Hecho Group turbidites (Van Lunsen, 1970; Ríos Aragués et al., 1982; Barnolas et al., 1991) (Fig. 3). This truncation, prior to the Boltaña anticline folding, is a slope feature of a foreland carbonate margin (Barnolas and Teixell, 1994) related to the drowning of the Boltaña shallow platform (Barnolas and Teixell, 1994) dated as Upper Ypresian by Mochales et al. (2012a).

The Hecho Group is made by siliciclastic turbidites and debris flows, carbonate debris sheets (megabeds) of shallow marine compounds, marls and marly-limestones. The age of the Hecho Group ranges from Upper Ypresian to Upper Lutetian (Labaume et al., 1985; Payrós et al., 1999; Oms et al. 2003; Gil-Peña et al., 2012). In the study area the younger turbidites are Middle Lutetian whereas the Middle to Upper Lutetian transition keeps yet into shallow marine deltaic facies. The age range in the study area is well established by the presence of the megabed 3 in the lower part of the section (Upper Ypresian after Labaume et al. 1985, Payrós et al. 1999, Gil-Peña et al., 2012) and the age of the San Felices turbiditic channel which is related to the lower part of the prograding Sobrarbe delta in the Ainsa area, where its Middle Lutetian age has been well established by Mochales et al. (2012a).

Over the San Felices turbiditic channel the sequence shallows quickly and a prograding deltaic sequence including nummulitic levels is recognised. This deltaic system belongs to the upper part of the Sobrarbe Fm. of the Ainsa basin (Puigdefàbregas, 1975; Dreyer et al. 1999). The age of deltaic Sobrarbe facies is Middle – Upper Lutetian (Mochales et al., 2012a). On the Sobrarbe Fm. a transitional to continental unit is recognised, followed by the continental facies of the Campodarbe Group (Fig. 3).

The Sobrarbe delta progrades to the N - NW in the Ainsa area, following the trend of N-

S folds. The continental sedimentation that followed from Late Lutetian onwards (Bentham, 1992; Mochales et al. 2012a) was initially fed by fluvial systems with a SE-NW orientation that turn rapidly to a E to W system fed by siliciclastic sediments sourced in alluvial fans located to the N, due to the uplift of northern area (Nijman and Nio, 1975; Puigdefàbregas, 1975). The Campodarbe Group (Bartonian-Oligocene) represents the mass re-distribution in the South Pyrenean Basin from the uplift related to the basement thrusting below the Gavarnie thrust, such as Bielsa and Guara-Gèdre (Fernández-Bellón et al., 2012; Muñoz et al., 2013; Izquierdo-Llavall et al., 2015). Thicknesses up to 4000 m of these molasse sediments are preserved to the West of the Boltaña anticline (Puigdefàbregas, 1975), in the core of the Guarga syncline (Figs. 2 and 3). Later stages of Oligocene deformation (Teixell, 1996; Fernández-Bellón et al., 2012), in relation to the Guarga basement thrust sheet emplacement, are recorded by tilting and folding of the Campodarbe Group and finally, of the Graus conglomerates (Sariñena Fm.; Quirantes 1978, Santolaria et al., 2015) southwards, in the front of the External Sierras.

2.2. Deformational stages

Within this tectono-stratigraphic frame, three different, non-coaxial episodes of deformation can be defined in the studied region:

A) The Gavarnie basement thrust emplacement during Lutetian-Bartonian times (Muñoz et al., 2013) probably extended to Bartonian-Oligocene (Séguret, 1972; Izquierdo-Lavall et al., 2015) is responsible for the reactivation/tilting of the thrust systems of the Internal Sierras (Larra, Monte Perdido) and the deformation of the turbiditic trough (Teixell, 1996). Frontal structures migrated southwards into the foreland, forming the first imbricate thrusts in the External Sierras (Millán et al., 2000).

The Balzes-Boltaña thrust sheet and related folds was emplaced during this time. Its oblique ramp in the northern sector, where the Boltaña anticline is located, connected NW-SE trending structures (i.e. Boltaña) with WNW-ESE Pyrenean structures. In the studied area, this is attestd by: i) the onlap of Hecho group turbidites on the eastern limb of the Boltaña anticline (Puigdefàbregas, 1975; Remacha et al., 2003), although part of this onlap is reported as prefolding (Rios-Aragués et al., 1982b; Muñoz et al., 2013); ii) by the thickness changes in the stratigraphic pile (Soto and Casas, 2001), specially towards the middle-upper part of the outcropping Hecho Group; iii) by the unstable slope lobes at the bottom of the San Vicente Fm. and iv) by the kinematics inferred from magnetic fabrics (Mochales et al., 2010) that display a remarkable change in the orientation of the stretching lineation. Balanced cross-sections (Fernández-Bellón et al., 2004; Muñoz et al., 2013) inform about the folding style of the northern sector of the Boltaña anticline: a west-verging thrust décolled in the Triassic evaporites cutting through the Cuisian pile and partially through the Hecho turbidites in the northern sector. The thrust surface propagates and finally disappears within the Eocene, and does not crop out at the present-day erosion level. Local deformation in the Jánovas area linked to the emplacement of the Boltaña-Balzes sheet includes tilting in the western limb of the Boltaña anticline and a set of anticlines and synclines to the SW (Fig. 5a)

B) Vertical axis rotation (VAR). According to Mochales et al., (2012b), the Boltaña anticline formed first with a NW-SE orientation and then rotated (VAR: 45-55°), in relation to the emplacement of coeval or younger thrusts in the Axial Zone developed in a piggyback sequence. The Bielsa and/or Guara-Gèdre thrust sheets, are likely responsible for moderate, post-emplacement rotations in the Internal Sierras (Izquierdo-Llavall et al., 2015). South of the study area, the rotation of the Boltaña anticline took place during the Lutetian (moderately) and more intensively during Bartonian to

Priabonian times, when its axis was positioned in the present N-S direction. However, Muñoz et al. (2013) argue that the Boltaña anticline development and VAR were synchronous from an initial stage of folding, when the anticline started with a NW-SE trend to the final folding stage, Late Lutetian to Late Bartonian. According to the different authors, rotational deformation is considered either partially coeval to folding and younger (Mochales et al., 2012b) or synchronous with folding during the entire process (Muñoz et al., 2013). In both interpretations, clockwise rotation affected the entire region changing the former trend of NW-SE structures to their present N-S orientation (Fig. 5b). This VAR is variable and very well constrained throughout the External Sierras and the Jaca Basin and seems to be related to a lateral gradient of the displacement or shortening (Pueyo, 2000; Soto et al., 2006; Muñoz et al., 2013). In the transition zone, at the western limb of the Boltaña anticline (Jánovas region), there is a sequence of folds with variable trends from WNW-ESE to N-S (Fig. 2a and Table 1) that are not associated with growth strata wedges and seem to postdate the growth of the Boltaña anticline (Fig. 5). This deformation style is due to the forelandwards progression of folding plus the re-arrangement caused by the Bartonian-Priabonian VAR. Changes along strike of the structures from N-S to NW-SE do not imply a superposition of these structures in time, but differential stages of deformational processes (Fig. 6).

C) Finally, the emplacement of the Guarga basement thrust is related to the main uplift of the Axial Zone, the propagation of thrusting towards the External Sierras via the Upper Triassic décollement (see Fig. 1), the formation of the Southern Pyrenean front, and the southwards displacement of the Jaca piggyback basin (Ori and Friend, 1984; Millán et al., 2000). Its emplacement has been constrained between Middle Rupelian and the Early Miocene (Teixell, 1996) (or the Early Rupelian, according to Fernández-

Bellón et al., 2012), contemporaneous with the upper part of the Campodarbe and Uncastillo-Sariñena Fms. It is responsible for the generation of both a large ramp in the External Sierras and the southwards tilting of the northern units (study area) caused by the forelimb geometry of the thrust, thus generating the WNW-ESE Guarga synclinorium (Puigdefàbregas, 1975; Teixell, 1996; Millán et al., 2006; Fernández-Bellón et al., 2012). Deformation in the Jánovas area produced tilting of earlier folds, related to the hanging wall ramp of the basement, increasing the plunge of the fold axes to the west of the Boltaña anticline (Fig. 5c). In the particular case of the studied area, there is superposition between folds formed in the previous stage and the Pyrenean trend imposed by the folding associated with the Guarga thrust.

In conclusion, the structures observed in the study area, both in the turbiditic and in the slope facies, would be caused by a superposition of different deformation episodes. At least two of them (folding consistent with uplift of the Boltaña anticline) and folding linked to the Guarga thrust, show non-coaxial folding directions, as can be demonstrated from the analysis of bedding orientation, both in the geological map and the stereoplots (Fig. 2). Their relationship with the intermediate, vertical axis rotation linked to the emplacement of the Boltaña anticline is controversial and beyond the scope of this work. As already mentioned, the issue of the temporal location of vertical-axis rotation with respect to the other two folding episodes does not affect the restoring of paleomagnetic vectors since VAR is commutative, and therefore its location within the sequence of events is not relevant for the restoration of paleomagnetic vectors associated with superposed folding.

3. PALEOMAGNETIC DATA

Thirteen new paleomagnetic sites (158 standard samples) were taken with a gas-powered drilling machine and oriented in-situ (Fig. 2a, Table 1) in the western flank of the Boltaña anticline and northern limb of the Guarga synclinorium (Jánovas area). Bedding strikes are variable depending on the position within the fold system (Fig. 2b, Table 1). The ages of the sampled rocks, ranging from C20r (Middle Lutetian) to C18r (Early Bartonian), were inferred from detailed magnetostratigraphy of the Ainsa Basin (Mochales et al., 2012a). Two sites from other authors (Pueyo, 2000) located in the Jánovas area were also considered here.

Detailed thermal demagnetizations (13-15 steps) were applied by means of 2G magnetometers and TDS-1 ovens at the Rome and Barcelona laboratories. Previous experience (Mochales et al., 2010 and 2012a and 2012b) in this kind of rocks helps optimising the cleaning sequence. Mineral neoformation precluded any further ChRM characterization over 500ºC. ChRM directions were fitted in the orthogonal diagrams using the principal component analysis method (Kirschvink, 1980), by means of the programs Paldir (Utrecht) and VPD (Ramón, 2013). Orthogonal diagrams show two imprints of the magnetic field: a low temperature and viscous component unblocking below 235ºC and a two-polarities ChRM isolated from 300 to 500ºC (Fig. 6).

Rock magnetism analyses were performed to control the carriers of the paleomagnetic signal. By means of the pulse magnetizer (2G at the Istituto Nazionale di Geofisica e Vulcanologia [INGV] in Rome) and 2G-cryogenic magnetometer, 13 samples were thermally demagnetized following Lowrie's test (1990); a 1.2 T field was applied to the z axis, 0.3 T to the x axis, and 0.1 T to the y axis. Subsequently, thermal stepwise demagnetization was applied up to 600 °C. Magnetization is mainly borne by magnetite with variable iron sulphides content, and exceptionally minor contents of hematite (Fig. 7), in agreement with previous rock magnetism essays in equivalent rock units

(Mochales et al., 2012a, b; Muñoz et al., 2013).

3.1. Paleomagnetic stability

The fold test performed with the new data shows a non-significant result (Fig. 8) although the grouping of the vectors is better after the total restoration to the paleo-horizontal. Apart form other possible sources of noise, this may be partially caused by the large scattering (banana-like shape) produced in declination due to the synrotational character of the data (according to the known rotation ages; Mochales et al., 2012b; Muñoz et al., 2013). As already pointed by Mochales et al. (2012a, b), the mean Eocene magnetic record (N035E) in the Ainsa Basin, as in the Jánovas area, may also account for the non-significant result of the fold test, because of the obliquity of the expected field and the fold axis. However, it is worth mentioning the constancy of the inclination and the similarity to the expected one (see next section and stereoplots in Fig. 8).

In any case, the primary origin of the magnetization in the area is attested by the occurrence of two polarities and it is endorsed by numerous paleomagnetic works in the South Pyrenean Basin (Pueyo et al., 2002, 2003b; Larrasoaña et al., 2004; Rodríguez-Pintó et al., 2013a and b; Muñoz et al., 2013).

3.2. Vertical Axis rotations in the Jánovas Region

The reference used in this work was calculated for the Aínsa Basin using the stable data from the Eastern Pyrenean foreland basin during Eocene times (profiles La Rovira and Grau de Sunyer of Vic area, Easterm Pyrenees); Declination: 004º, Inclination: 53º, a95: 4.6°, k: 9.6 (Taberner et al, 1999). The reference paleomagnetic direction in the study area was finally defined according to the following steps and data input:

i) Geographic coordinates (foreland data); Latitude: 41° 55’ N (41.92°), Longitude: 2°,

15'E (2.25°)

ii) Paleomagnetic mean: n:110 (67N+43R) N+(-R); Dec: 004.2; Inc: 52.6; α95: 4.6°, k: 9.6 (Taberner et al, 1999).

iii) The Virtual Paleomagnetic Pole calculation was done by means of the program VGP.exe (University of Utrecht). The VGP coordinates of the derived pole are: PLat: 80.7; PLong: 155.6E

iv) Geographic coordinates (Ainsa area); Latitude: 42° 21' N (41.35°), Longitude: 0°, 04'E (2.07°). This position represents the central part of the studied area.

The reference paleomagnetic direction of the study areas is: n:110 (67N+43R) N+(-R); Dec: 004.6; Inc: 53.2; α95: 4.6°, k: 9.6.

The angular differences between the declination of this reference and our sites are the Vertical Axis Rotations (VAR) observed in every site. Discrete VAR data derived from four previous sites (LIG1 and LIG2 by Pueyo, 2000) have been taken into account (Table 1 and Fig. 2a)

4. FOLD TREND ANALYSIS IN THE JÁNOVAS REGION

When considering sequential restoring, a fundamental step is the determination of the trend and plunge of the structures involved. Complementarily to the detailed analysis of bedding orientation in the Jánovas sector (see below), we have performed a detailed geometric analysis of the trends of the fold axes in all surrounding structures (Fig. 9):

- The Boltaña anticline axis is subhorizontal and shows a N004E trend (Mochales et al., 2010).

- To the South, the Guarga syncline (easternmost portion of the Guarga synclinorium)

shows one of the characteristic Pyrenean trends in the occidental region (N112E) (Larrasoaña et al., 1997; Pueyo, 2000; Izquierdo-Llavall et al., 2013).

- More to the South, the northern sector of the Balzes anticline (in the External Sierras) shows a N006E trend (Rodríguez-Pintó et al., 2015), similar to the Boltaña anticline, although it exhibits a slightly steeper plunge to the North (8°).

- The large cartographic features to the West (Basa anticline and Orosia syncline) display trends of N117E and N107E respectively (Larrasoaña et al., 1997; Pueyo, 2000). These two folds progressively acquire steeper plunges to the East, where the Jánovas sector is located. Map-view features attest for the superposition of these two distinct structural trends (the N-S and the Pyrenean one) in the studied region (Fig. 9).

A finer analysis of bedding orientation was conducted to unravel geometric features in the Jánovas sector in the western flank of the Boltaña anticline. Bedding data were acquired during fieldwork or compiled from previous maps (Barnolas et al., in press; Muñoz et al., 2013) with the aim of deciphering the trend and plunge of the folds in this complex area. Axial planes can be tentatively defined by means of numerous bedding measurements and three distinct folds, apart from Boltaña, can be tracked from East to West: San Felices (N246E,44), Planillo (N257E,52) and Arbella (N231E,52) (see Fig. 2 for Bingham statistics of the bedding poles). Fold axes are roughly coplanar, according to a SW-dipping plane (Fig. 10). This fact and the strong plunging of the axes support the existence of a tectonic episode of tilting with NW-SE strike, postdating the formation of the three folds. In our interpretation, this younger deformation event must be related to the Guarga thrust.

5. PALEOMAGNETIC RESTORATION: DISCUSSION.

In areas of tilted bedding we can assume either the axis of tilt and calculate a paleomagnetic pole from the tilt-corrected vector, or the paleomagnetic direction, from a coeval pole for the plate, and determine the axis of rotation or tilt (MacDonald, 1980). In this latter case, we assume a paleomagnetic direction from the reference for this age at this particular point of the plate (Eocene in our case, Taberner et al, 1999) and we understand VAR as the difference in declination between the reference and the local paleomagnetic orientation. It is sometimes overlooked that the bedding tilt correction involves an assumption, regarding the orientation of the tilt axis, that directly establishes the position of the paleomagnetic pole calculated from the corrected vector. In the same way, with the aim of determining the orientation and plunge of fold axes, we have measured and gathered more than one hundred bedding orientations and proceeded to sequential restoration to unravel how these fold axes change in orientation during the restoration process (Fig. 10).

Surveyed sites for paleomagnetic studies were gathered depending upon their structural position, to control VAR changes across the study area. They have been grouped in three sectors according to the structural analysis: eastern (A and B domains, San Felices syncline); central (B and C domains, Planillo anticline) and western (C and D domains, Arbella syncline) (Fig. 2; Tables 1 and 2).

We consider the existence of these three phases since previous studies (Mochales et al., 2010; Mochales et al., 2012b) performed in the Boltaña anticline indicate the nucleation of the fold in early-middle Lutetian times by means of AMS data and considering the onlap predating previous to the middle Lutetian unconformity as the beginning of folding. A detailed chronostratigraphy allow us to estimate the age of the formations involved in this study, being able to determine different rotation rates: slow rotational pace during Lutetian times (1º/M.a.), increasing between Late Lutetian-Bartonian

(2.6º/M.a.), and dramatically increasing during Bartonian-Priabonian ages (up to 10º/M.a.) (Mochales et al., 2012b). Other authors have tackled this problem (Muñoz et al. 2013), and propose synchronous folding and VAR during Late Lutetian to Late Bartonian. The third stage proposed, that is, the tilting associated with the emplacement of the basement Guarga thrust, is clearly defined, both in relative chronology and basement structure, in several cross-sections, especially those located west of the studied area (Teixell, 1994; Casas and Pardo, 2004; Izquierdo-Llavall et al., 2013). The along-strike prolongation of the Guarga thrust towards the East of the study area has also been pointed out (Martínez-Peña and Casas-Sainz, 2003), and can be correlated with the basement thrust sheets defined along the ECORS-Pyrenees cross-section (Muñoz, 1992). Other indicators, such as extensional faults that run parallel to the Boltaña anticline, are consistent with this deformational sequence. These faults have been interpreted as (i) developed before thrusting and folding in the peripheral bulge area of the foreland due to outer-arc extension and (ii) subsequently rotated 70º CW (Tavani et al., 2012). However, the orientation of these faults could have initially been NW-SE, oblique to the future axis of the Boltaña anticline, because of the orientation of the forebulge itself, conditioned in its turn by (i) the migration of deformation from E to W during the Pyrenean orogenesis (Millán et al., 2000) and (ii) the also oblique orientation of the basal thrusts with respect to the typical WNW-ESE Pyrenean trend (Martínez-Peña and Casas-Sainz, 2003). According to this interpretation, this set of extensional faults would be consistent with the n 45º VAR obtained from paleomagnetic data by Mochales et al. (2012b). Another controversial point is how much of the tilt in the Eocene beds observed at surface is related to the Guarga thrusting and how much of this tilting is related to the emplacement of previous thrust sheets (Bielsa/Guara-Gèdre and Gavarnie, see cross-section of Fig. 1; see also equivalent sections performed by

Millán et al., 2006 and Meresse, 2010). Regardless of this quantitative question (that, on the other hand, does not affect the calculations and the method of restoration proposed), this three-step evolution can be used as a working hypothesis for unravelling the orientation of paleomagnetic vectors. Although interaction between the three described processes may exist (see, e.g. Muñoz, 2014), and probably superimposed during particular time intervals, their simplification into three stages allow for a direct translation into mathematical/geometrical calculations that also permit a feedback with thrust sequences defined from geological indicators.

5.1. Sequential restoration in superposed folding.

A correct restoration of the paleomagnetic data must follow the reverse sequence of deformation events, firstly removing the younger deformation (Guarga tilting) to finally unfold the remaining dip and paleomagnetic vectors till definitive restitution (deformation related to the Gavarnie thrust). Nevertheless the commutative character of the VAR would allow us to remove the rotational value to the former state, at any stage of the restoration, with totally equivalent results (Pueyo, 2000). In this way, we will achieve a true restoration to the paleogeographic reference system and the difference with the paleomagnetic reference will be the real VAR (in contrast to other spurious components caused by incorrect restoration procedures; MacDonald, 1980; Pueyo, 2000). For the first restoration step, the final tilting of beds with Pyrenean direction must be considered. The maximum tilt of Upper Eocene-Lower Oligocene beds in the Guarga syncline is at present 55º S as depicted in the cross-sections presented in this paper (Fig. 1c), and also shown in sections by Millán et al (2006) and Meresse (2010). An agreement exists in those sections about the dip of the forelimb (≈ 30°) of the corresponding Guarga basement thrust at depth. In our interpretation, all the tilting observed in the Cenozoic cover can be specifically associated with the Guarga basement

thrust. Although it can be argued that some part of this tilting could be related to former basement thrusting stages (either Bielsa/Guara-Gèdre or Gavarnie), especially for the marine sediments within the sequence (see cross-section in Fig. 1), the relative parallelism of bedding throughout the sedimentary pile allows to consider a post-Eocene origin for the tilting of this limb. Furthermore, the possibility of an older origin of part for this tilting , that was inferred from geological mapping features (Puigdefàbregas, 1975) in the vicinity of the study area, would not alter the calculations of VAR.

Fold axes in the Jánovas oblique zone (San Felices, Planillo and Arbella folds) become subhorizontal, with cylindrical geometry, after removing the Guarga tilting (almost completely horizontal if the 55° S, end-member Guarga tilting is considered). At this state, after Guarga correction, the fold axes in the Jánovas superposed zone fall between N040E-N060E (Figure 10). These trends are almost perpendicular to the Pyrenean axes of Guarga, Oturia or Basa folds, whose axes have kept similar trends to their pre-tilting orientation since they are coaxial with the tilting axis. Given that VAR are commutative, the remaining restoration step consists in rotating back the bedding to the horizontal according to a horizontal axis (Fig. 10). The angle between the obtained orientation for the paleomagnetic vector and the reference will then be the value of VAR for each site.

Starting from the non-corrected data (bac), sequential restoration shows an evident variation of the VAR from E to W, depending of the restoration method. Direct restoration (bedding correction) is classically used in many paleomagnetic studies (abc), where vectors are restored to undeformed stage by means of rotating around the strike of bedding (Table 2 and Fig. 11b). Gathered by folds, direct restoration presents VAR values of 48º (α_{95}: 39.4°) at San Felices syncline; 30º (α_{95}: 14.8°) at Planillo anticline; 30º (α_{95}: 10.3°) at Arbella syncline. Sequential restoration is here divided into partial restitution, after the removal of the regional bedding (aGc, i.e. tilting associated with the

Guarga thrust) and total restitution (aTc, after removing the first folding stage) (Table 2 and Fig. 11c). Besides, two tilting magnitudes have been considered. Gathered by folds, at the intermediate stage of restitution (aGc) VAR values are 37-38º (α_{95}: 52.1°) at San Felices syncline; 32-33º (α_{95}: 16.2°) at Planillo anticline; 29-32º (α_{95}: 10.3°) at Arbella syncline. The total restitution (aTc) provides values of the true VAR undergone in the region between 53-56º (α_{95}: 13.0°) at San Felices syncline; 29-27º (α_{95}: 19.7°) at Planillo anticline and 24-20º (α_{95}: 9.8°) at Arbella syncline (aTc in Table 2 and Fig. 11). These variations, based on significant differences of VAR, can be related to the diminishing influence of the rotation linked to the Boltaña area towards the West.

5.2. Bedding correction and error analysis.

Simple bedding correction also indicates a gradual but moderate decrease in rotation means from E to W: 49º (α_{95}: 39.4°) for the San Felices syncline, 31º (α_{95}: 14.8°) for Planillo anticline, and 31º (α_{95}: 10.3°) for the western Arbella syncline (abc in Table 2 and Fig. 11a). Previous data in the hanging wall of the Boltaña thrust (ARA sites from Mochales et al. 2012b) display similar rotation values (42° +/- 6°). Taking into account the confidence angles, they could fit into the expected rotation value. However, stronger internal scattering in all sectors arises when superposed folding is not taken into account. Comparing the results, the sequential restoration seems to give more consistent and confident results since in the Arbella and San Felices synclines error angles have been reduced, slightly in the first case and considerably in the second (Fig. 12). An important increase of the error angles when applying the simple bedding correction is observed in most cases (Table 1), particularly in San Felices syncline sector (almost 30°) and requires a deeper discussion. Here, one of the sites (JAN1) records -30° of apparent rotation in one of the flanks, whereas the other flank (two sites; SFE2 and SFE3)

records up to +41° of error. In the case of Arbella syncline, it presents a better-defined clustering and a moderate decreasing of the α_{95} angle (≈0.5°). Nevertheless, in the case of Planillo anticline, the defined clustering (α95 angle) remains the same independently of the restoration performed. In general, VARs derived from simple bedding correction are higher (except for the Planillo anticline), in absolute value, than those coming from the sequential restoration (Fig 12a), and the error is biased towards a positive sign (an spurious clockwise rotation). The difference between them (error) is larger for increasing magnitudes of VARs, although this is controlled by their structural location (Pueyo, 2000; Ramón, 2013). Data correction in the San Felices syncline largely improves with the sequential restoration; its uncertainty (α95) decreases 26º (Fig. 11 and Table 2). The simple restoration would yield an average of 33º CW for the entire Jánovas sector (Fig. 12) with the considerable overlapping of α95 cones that would prevent establishing any other structural consideration (abc in Fig. 12b and Table 2). On the contrary, the sequential restoration reduces the sector errors (α95) and allows observing the geographic change of rotations in relation to the fold trends. The eastern San Felices syncline would record ≈ 55º CW rotations, progressively decreasing towards the west, with ≈ 30º CW in the case of the Planillo anticline and ≈25º CW for the Arbella anticline (aTc in Fig. 12b and Table 2). This decrease is independent of the fold trend, that remains similar for the three folds, and can be interpreted as a consequence of gradual, westwards-decreasing influence of the rotational pattern characteristic of this sector of the Central Pyrenees, that would not then be exclusively linked to the formation of the Boltaña anticline but also to other underlying thrusts (Mochales et al., 2012b). This is also suggested by the independence between latitude (distance along the fold) and displacement of thrusts underlying the Boltaña anticline. The relationship between the Jánovas fold system and rotation cannot be deciphered

from paleomagnetic data, although growth strata relationships (see Fig. 4) point to a younger stage with respect to the Boltaña anticline and possibly linked to rotational kinematics.

CONCLUSIONS

In this paper we deal with the problem of restoration of paleomagnetic vectors in areas of superposed folding. We present 15 new paleomagnetic sites from a complex area located in the western limb of the Boltaña anticline (Southern Pyrenees).

We have considered three stages of deformation, taking into account published data (Mochales et al., 2012b) that indicate a diachronism between folding (Lutetian in age) and a main rotational event during Bartonian-Priabonian. Consequently, we distinguished stages of i) folding of the Boltaña anticline ; ii) rotation of the Boltaña anticline, that acquired its present-day N-S orientation and formation of the Jánovas fold system; iii) tilting with Pyrenean trend linked to the Guarga thrust. According to Muñoz et al. (2013), the stages of folding and rotation would be coeval, defining the fan-shape in map view of the Jánovas fold system since early stages. In both cases (either considering two or three deformational stages), the result of sequential restoration is equivalent from the paleomagnetic point of view that, in this case cannot help to distinguish between the two interpretations..

The comparison between simple bedding correction and the sequential restoration (according to the reverse order of deformational processes) allow to reach the following conclusions:

The errors affecting the VAR magnitude are 13° (clockwise) in average, although they

range between -30° and +41° in some sites. This increases up to 27º the α_{95} confidence angle in one out of the three structural sectors (grouping of sites). These magnitude and sense of the errors are controlled by structural position of sites.

The sequential restoration considering all the deformational stages highlights VAR variations of 40º, that decrease (in a tentative calculation) in a narrow area with a rate of 10º/ km from East to West.

Finally, this example shed some light on the little-explored field (from the paleomagnetic point of view) of areas undergoing sequential folding processes, especially in complex zones with displacement transfer between structures. Moreover, sequential restoration on the basis of regional data reveals itself as an adequate mean to understand possible scattered vectors, allowing for reducing error reduction. This provides a deeper analysis of paleomagnetic data and consequently helps understanding the actual kinematics of mountain belts.

ACKNOWLEDGEMENTS

This work was sponsored by a fellowship from the Geological Survey of Spain (IGME). Research financial support comes from the projects Pmag3Drest (CGL-2006-2289-BTE MEC, CGL2009-14214 and CGL2008-00809/BTE MICINN), ChronoPyr (IGME-346) and 3DR3 (PI165/09 Gob. Aragón). Bases Europa (CAI-DGA) funded the Rome stay. We are very grateful to B. Beamud and E. Costa (Barcelona), F. Speranza and M. Maffione (Rome) for support and advices offered to this work. We are especially grateful to J. Ramajo for his mapping advice. V. Lafuente and P. L. Mochales helped during fieldwork. We sincerely appreciate the constructive review done by Josep Antón

Muñoz and Stefano Tavani who helped us to improve this work. Stereoplots were made using "Stereonet" program (6.3.3) by Richard Allmendinger (Allmendinger,et al., 2012; Cardozo and Allmendinger, 2013) to whom we are very grateful.

REFERENCES

Allerton, S., 1998. Geometry and kinematics of vertical-axis rotations in fold and thrust belts. Tectonophysics 299, 15-30.

Allmendinger, R.W., Cardozo, N., Fisher, D.M., 2012. Structural Geology Algorithms: Vectors and Tensors. Cambridge University Press.

Anastasio D.J., Holl, J.E., 2001. Traverse fold evolution in the External Sierra, southern Pyrenees. Journal of Structural Geology. 23, (2-3), 379-392.

Barnolas, A., Samsó, J.M., Teixell, A., Tosquella, J., Zamorano, M., 1991. Evolución sedimentaria entre la cuenca de Graus-Tremp y la cuenca de Jaca-Pamplona. I Congreso del Grupo Español del Terciario. Libro-Guía de la excursión nº 1, EUMO Gràfic, Vic, 123 p.

Barnolas A., Teixell, A., 1994. Platform sedimentation and collapse in a carbonate-dominated margin of a foreland basin (Jaca basin, Eocene, southern Pyrenees). Geology, vol. 22, no 12, 1107-1110.

Barnolas, A.; Montes, M.; Malagón, J.; Gil-Peña, I., Rico, M. (in press).- Mapa geológico y memoria de la Hoja nº 211, Boltaña, del Mapa Geológico de España a escala 1:50.000 (MAGNA). Instituto Geológico y Minero de España, Madrid.

Beamud, B., 2013. Paleomagnetism and Thermochronology in Tertiary syntectonic

sediments of the South-central Pyrenees: chronostratigraphy, kinematic and exhumation constraints. Unpublished PhD Universitat de Barcelona.251 p.

Bentham, P.A., 1992. The tectono-stratigraphic development of the western oblique ramp of the south-central Pyrenean thrust system, Northern Spain. Ph.D Thesis. University of Southern California. 253.

Bingham C., 1974. An antipodally symmetric distribution on the sphere. Annals of Statistics 2, 1201-1225.

Bond, R. M. G., McClay, K. R., 1995. Inversion of a Lower Cretaceous extensional basin, south central Pyrenees, Spain. In. Basin inversion (J.G Buchanan, P.G. Buchnan, Eds.), Geological Society Special Publication, 88, 415-431.

Borradaile G.J., 1997. Deformation and paleomagnetis. Surv. Geophys, 18, 405-435.

Cámara, P., Klimowitz, J., 1985. Interpretación geodinámica de la vertiente centro-occidental surpirenaica (Cuencas de Jaca-Tremp). Estudios geológicos, 41, 391–404.

Cardozo, N., Allmendinger, R.W., 2013. Spherical projections with OSXStereonet. Computers & Geosciences 51 (2013) 193–205.

Dinarès-Turell J., McClelland, E., Santanach, P., 1992. Contrasting rotations within thrust sheets and kinematics of thrust tectonics as derived from palaeomagnetic data: an example from Southern Pyrenees. In: Thrust tectonics (K.R. McClay Ed.), Chapman and Hall, London, 265-275.

Dreyer, T., Corregidor, J., Arbues, P., Puigdefàbregas, C., 1999. Architecture of the tectonically influenced Sobrarbe deltaic complex in the Ainsa Basin, northern

Spain: Sedimentary Geology, 127, 127-169.

Farrell S.G., Williams G.D., Atkinson C.D., 1987. Constraints on the age of movement of the Montsech and Cotiella thrusts, south central Pyrenees, Spain. Journ. Geol. Soc. of London, 144: 907-914.

Fernández-Bellón, O., 2004. Reconstruction of geological structures in 3D. An example from the Southern Pyrenees. Ph.D Thesis. Universitat de Barcelona. 321.

Fernández-Bellón, O., Muñoz, J.A., Arbués, P., Falivene, O., Marzo, M., 2004. Three-dimensional reconstruction of geological surfaces: an example of growth strata and turbidite systems from the Ainsa Basin (Pyrenees, Spain). American Association of Petroleum Geologists Bulletin 88(8), 1049–1068.

Fernández-Bellón, O., Muñoz, J.A., Arbués, P., Falivene, O., 2012. Structure and evolution of an oblique system of relaying folds: The Ainsa basin (Spanish Pyrenees), Journal of the Geological Society of London, 169, 545-559, doi: 10.1144/0016-76492011-068.

Fisher, R. A., 1953. Dispersion on a sphere, Proc. R. Soc. London, Ser. A, 217, 295 – 305.

García-Senz, J., 2002. Cuenca extensivas del Cretácico Inferior en los Pirineos Centrales, formación y subsecuente inversión. Ph.D Thesis. Universidad de Barcelona.

Garrido-Mejías, A., 1973. Estudio geológico y relación entre tectónica y sedimentación del secundario y terciario de la vertiente meridional pirenaica en su zona central. Ph.D Thesis. Universidad de Granada. 395 p.

Gil-Peña, I., Barnolas, A., Montes-Santiago, M, García-Ruiz, J.M., Peña-Monné, J.L., Martí-Bono, C, Gómez-Villar, A., 2012, Memoria de la Hoja nº 177 (Sabiñánigo) del mapa geológico 1:50.000 de España (MAGNA). IGME, Madrid, 82 pp.

Holl J.E., Anastasio D.J., 1995a. Cleavage development within a foreland fold and thrust belt, southern Pyrenees, Spain. Journal of Structural Geology. 17; 3, 357-369.

Holl, J.E., Anastasio, D.J., 1995b. Kinematics around a large-scale oblique ramp, southern Pyrenees, Spain. Tectonics. 14; 6, 1368-1379.

Kirschvink, J.L., 1980. The least-squares line and plane and the analysis of paleomagnetic data: Geophysical Journal. Royal Astronomical Society, 62, 699-718.

Kodama, K. P. 1988. Remanence rotation due to rock strain during folding and the stepwise application of the fold test. Journal of Geophysical Research, B, Solid Earth and Planets. 93; 4, Pages 3357-3371.

Kodama, K.P., 1997. A successful rock magnetic technique for correcting paleomagnetic inclination shallowing: Case study of the Nacimiento Formation, New Mexico, J. Geophys. Res., 102, 5193-5206.

Labaume, P., Séguret, M., Seyve, C., 1985. Evolution of a turbiditic foreland basin an analogy with an accretionary prism: Example of the Eocene South-Pyrenean basin. Tectonics, 4 (7), 661-685.

Larrasoaña, J.C.; E.L Pueyo; H. Millán; J.M. Parés; J. del Valle., 1997. Deformation mechanism deduced from AMS data in the Jaca-Pamplona basin (Southern

Pyrenees). Physics and Chemistry of the Earth, 22(1-2), 147 -152.

Larrasoaña, J. C.; Pueyo, E. L.; Parés, J. M., 2004. An integrated AMS, structural, palaeo- and rock-magnetic study of the Eocene marine marls from the Jaca-Pamplona basin (Pyrenees, N Spain); new insights into the timing of magnetic fabric acquisition in weakly deformed mudrocks. Magnetic Fabric: Methods and Applications (Edited by: Martín-Hernández, F., Lüneburg, C. M., Aubourg, C. & Jackson, M.). Geological Society of London Special Publication 238, 127 – 144.

Lowrie, W., Hirt, A.M., Kligfield, R., 1986. Effects of tectonic deformation on the remanent magnetizaton of rocks, Tectonics **5**, 713–722.

Lowrie, W., 1990. Identification of ferromagnetic minerals in a rock by coercivity and unblocking temperature properties. Geophys. Res. Lett., 17, 159-162.

MacDonald, 1980. Net tectonic rotation, apparent tectonic rotation, and the structural tilt correction in paleomagnetic studies. Journal of Geophysical Research, v. 85, p. 3659-3667.

Martínez-Peña, M.B., Casas-Sainz, A., 2003. Cretaceous-Tertiary tectonic inversion at the Cotiella Nappe (Southern Pyrenees, Spain). Int. J. Earth Sci. (Geol. Rundschau), 92, 99-113.

McCaig, A. M., McClelland, E., 1992. Palaeomagnetic techniques applied to thrust belts. In: Thrust Tectonics, (Ed. by K.R. McClay), 209-216, Chapman Hall Eds., London. 447 p.

MacDonald, W. D., 1980. Net tectonic rotation, apparent tectonic rotation, and the structural tilt correction in paleomagnetic studies. Journal of Geophysical Research: Solid Earth (1978–2012), 85(B7), 3659-3669.

Mencos, J., 2010. Metodologies de reconstrucció i modetització 3D d'estructures geològiques: anticlinal de Sant Corneli-Bóixols (Pirineus centrals). Doctoral dissertation Universitat de Barcelona.

Meresse, F., 2010. Dynamique d'un prisme orogénique intracontinental: évolution thermochronologique (traces de fission sur apatite) et tectonique de la Zone Axiale et des piémonts des Pyrénées centro- occidentales (Doctoral dissertation, Université de Montpellier 2). https://tel.archives-ouvertes.fr/tel-00772154/document.

Millán, H., 1996. Estructura de las Sierras Exteriores Aragonesas. Ph. D. Thesis. Universidad de Zaragoza, 213 p.

Millán, H., Pueyo, E., Aurell, M., Luzón, A., Oliva, B., Martínez-Peña, B., and Pocoví, A., 2000. Actividad tectónica registrada en los depósitos terciarios del frente meridional del Pirineo central, Rev. Soc. Geol. Esp., 13, 279 – 300.

Millán, H., Oliva-Urcia, B., & Pocoví-Juan, A., 2006. La transversal de Gavarnie-Guara. Estructura y edad de los mantos de Gavarnie, Guara-Gèdre y Guarga (Pirineo centro-occidental). Geogaceta, (40), 35-38.

Mochales, T., 2011. Chronostratigraphy, vertical axis rotations and AMS in the Boltaña anticline (Southern Pyrenees): Kinematic implications. Unpublished PhD Thesis. University of Zaragoza. 222 p. http://zaguan.unizar.es/record/6269

Mochales, T.; Pueyo, E.L.; Casas, A.M.; Barnolas, A.; Oliva-Urcia, B., 2010. Anisotropic magnetic susceptibility record of the kinematics of the Boltaña Anticline (Southern Pyrenees). Geol. J. 45: 562-581. DOI: 10.1002/gj.1207

Mochales, T.; Barnolas, A.; Pueyo, E.L.; Casas, A.M.; Serra-Kiel, J.; Samsó, J. M.; J.

Ramajo; Sanjuán, J., 2012a. Chronostratigraphy of the Boltaña anticline and the Ainsa Basin (Southern Pyrenees). Geological Society of American Bulletin, 124 (7-8), 1229-1250.

Mochales, T.; Casas, A.M.; Pueyo, E.L.; Barnolas, A., 2012b. Rotational velocity for oblique structures (Boltaña anticline, southern Pyrenees). Journal of Structural Geology 35, 2-16.

Muñoz, J.A., 1992. Evolution of a continental collision belt: ECORSPyrenees crustal balanced cross-section. In: Thrust Tectonics (K.R. McClay Ed.), Chapman and Hall: London; 235–246.

Muñoz, J.A., Coney, P.J., McClay, K.R., Evenchick, C.A., González, A., Arenas, C., Pardo, G., 1997. Discussion on syntectonic burial and post-tectonic exhumation of the southern Pyrenees foreland fold-thrust belt. J. Geol. Soc. London, 154, 361-365.

Muñoz, J. A., Beamud, E., Fernández, O., Arbués, P., Dinarès‐Turell, J., & Poblet, J., 2013. The Ainsa Fold and thrust oblique zone of the central Pyrenees: Kinematics of a curved contractional system from paleomagnetic and structural data. Tectonics, 32(5), 1142-1175.

Mutti, E., 1977. Distinctive thin-bedded turbidite facies and related environments in the Eocene Hecho Group (south-central Pyrenees, Spain). Sedimentology. U:107-131.

Nijman, W., Nio, S.D., 1975. The Eocene Montañana delta. In: Sedimentary evolution of the Paleogene South Pyrenean Basin (J. Rosell, C. Puigdefabregas, Eds.), IAS 9th International Congress, Nice, part B, 56 p.

Oliva-Urcia, B.; Pueyo, E. L., 2007. Rotational basement kinematics deduced from remagnetized cover rocks (Internal Sierras, Southwestern Pyrenees). Tectonics 26 TC4014, doi: 10.1029/2006TC001955.

Oliva-Urcia, B.; Casas, A. M.; Pueyo, E. L.; Pocoví, A., 2012. Structural and paleomagnetic evidence for non-rotational kinematics in the western termination of the External Sierras (southwestern central Pyrenees). Geologica Acta, 10 (2), 125-144.

Oms, O., Dinarès-Turell, J.; Remacha, E., 2003. Magnetic stratigraphy from deep clastic turbidites: an example from the Eocene Hecho group (southern Pyrenees). Studia Geophysica et Geodaetica, 47(2), 275-288.

Ori G. G., Friend P. F., 1984. Sedimentary basins formed and carried piggyback on active thrust sheets. Geology 12:475–478.

Parés, J. M., Dinarès, J., 1993. Magnetic fabric in two sedimentary rock types from the Southern Pyrenees. J. Geomag. Geoelectr. 45, 193–205.

Pastor-Galán, D., Gutiérrez-Alonso, G., Mulchrone, K. F., & Huerta, P., 2012. Conical folding in the core of an orocline. A geometric analysis from the Cantabrian Arc (Variscan Belt of NW Iberia). Journal of Structural Geology, 39, 210-223.

Payrós, A., Pujalte, V., Orue-Etxebarria, X., 1999. The South Pyrenean Eocene carbonate megabreccias revisited: new interpretation based on evidence from the Pamplona basin. Sedimentary Geology, 125, 165-194.

Poblet, J., Hardy, S., 1995. Reverse modelling of detachment folds; application to the Pico de Aguila anticline in the South Central Pyrenees (Spain). Journal of Structural Geology, 17, 1707-1724.

Poblet, J., Muñoz J.A., Travé A., Serra-Kiel J., 1998. Quantifying the kinematics of detachment folds using three-dimensional geometry: Application to the Mediano Anticline (Pyrenees, Spain). Geological Society of America Bulletin 110: 111-125.

Pueyo, E.L., 2000. Rotaciones paleomagnéticas en sistemas de pliegues y cabalgamientos. Tipos, causas, significado y aplicaciones (ejemplos del Pirineo Aragonés). Ph.D Thesis. Universidad de Zaragoza. 296.

Pueyo, E. L.; 2010. Evaluating the paleomagnetic reliability in folds and thrust belt studies. Trabajos de Geologia 30 (1), 145 -154

Pueyo, E.L., Millán, H., Pocoví, A., 2002. Rotation velocity of a thrust: a paleomagnetic study in the External Sierras (Southern Pyrenees). Sedimentary Geology, 146, 191-208, doi: 10.1016/S0037-0738(01)00172-5.

Pueyo E.L., Parés, J.M., Millán, H., Pocoví, A., 2003a. Conical folds and apparent rotations in paleomagnetism (a case study in the Pyrenees). Tectonophysics, 362 (1/4): 345 366.

Pueyo E.L., Pocoví, A., Parés, J.M., Millán, H., Larrasoaña. J.C., 2003b. Thrust ramp geometry and spurious rotation of paleomagnetic vectors. Studia Geophysica Geodetica, 47: 331-357.

Pueyo, E.L., Pocoví, A., Millán, H., Sussman, A.J., 2004. Map-view models for correcting and calculating shortening estimates in rotated thrust fronts using paleomagnetic data, In: Orogenic Curvature: Integrating Paleomagnetic and Structural Analyses (A.J. Sussman, A.B. Weil Eds.), Geological Society of America Special Paper 383, p. 57-71.

Pueyo, E. L., Cifelli, F., Sussman, A. J. & Oliva-Urcia, B. (eds) Palaeomagnetism in Fold and Thrust Belts: New Perspectives. Geological Society, London, Special Publications 425, http://doi.org/10.1144/SP425.13

Puigdefàbregas, C., 1975. La sedimentación molásica en la cuenca de Jaca. Pirineos 104, 1–188.

Quirantes, J., 1978. Estudio sedimentológico y estratigráfico del Terciario continental de Los Monegros. Institución Fernando el Católico (CSIC), Tesis Doctorales, 27, 207 p.

Ramón, M.J., 2013. Flexural unfolding of complex geometries in fold and thrust belts using paleomagnetic vectors. Unpublished PhD University of Zaragoza, 228 p. http://zaguan.unizar.es/record/11750

Ramón, M.J.; Pueyo, E. L.; Briz, J. L.; Pocoví, A.; Ciria, J. C., 2012. Flexural unfolding in 3D using paleomagnetic vectors. Journal of Structural Geology, 35; 28-39

Remacha, E., Oms, O., Fernández, L.P., Crumeyrolle, P., Pettingill, H., Vicente, J.C., Suarez, J., Gual, G., Bolaño, F., Arcuri, M., Climent, F., 2003. Sand-rich Turbidite Systems and Megaturbidites of The Hecho Group from slope to the basin plain. Facies, stacking patterns, controlling factors and diagnostic features. AAPG International Conference and Exhibition, excursion num. 12, Field Guides 1 and 2, Barcelona.

Ríos-Aragués,L.M., Lanaja,J.M. Ríos-Mitchell, J.M., 1982a. Mapa Geológico de España 1/50000, Hoja 31-9 Bielsa. Mapa desplegable y Memoria explicativa, 48 p, IGME, Madrid.

Rios-Aragués L.M., Lanaja, J.M, Frutos, E., 1982b. Mapa Geológico de España

1:50.000, Hoja 178 Broto. Mapa y memoria explicativa, 60 p., IGME, Madrid.

Rodríguez-Pintó, A.; Ramón, M. J.; Oliva-Urcia, B.; Pueyo, E. L.; Pocoví, A., 2011. Errors in paleomagnetism: Structural control on overlapped vectors, mathematical models. Physics of the Earth and Planet. Interiors, 186; 11- 22

Rodríguez-Pintó, A.; Pueyo, E. L.; Pocoví, A.; Ramón, M. J.; Oliva-Urcia, B., 2013a. Structural control on overlapped paleomagnetic vectors: A case study in the Balzes anticline (Southern Pyrenees). Physics of the Earth and Planetary Interiors, 215, 43–57.

Rodriguez-Pintó, A.; Pueyo, E.L.; Serra-Kiel, J.; Barnolas, A.; Samsó, J. M.; Pocoví, A., 2013b. The Upper Ypresian-Lutetian in the San Pelegrín section (Southwestern Pyrenean Basin): magnetostratigraphy and larger foraminifera correlation. Palaeogeography, Palaeoclimatology, Palaeoecology 370, 13–29. doi: 10.1016/j.palaeo.2012.10.029

Rodríguez-Pintó, A.; Pueyo, E. L.; Sánchez, A.; Calvin, P.; Ramajo, J.; Casas, A. M.; Ramón, M.J.; Pocoví, A.; Barnolas, A.; Román-Berdiel, M.T. (reviewed). Rotational kinematics of a curved fold: the Balzes anticline (Southern Pyrenees). Tectonophysics.

Rosenbaum, G., Lister, G.S. and Duboz, C., 2002. Relative motions of Africa, Iberia and Europe during alpine orogeny. Tectonophysics, 359, 117-129.

Santolaria, P., Luzón, A., Casas, A. M., and Soto, R. (2015). Coupling far and near tectonic signals in syn-orogenic sediments: the Olvena growth strata (Sierras Marginales, Southern Pyrenees). Geologica Acta, 13(4). DOI: 10.1344/GeologicaActa 2015.13.4.3

Séguret, M., 1972. Étude tectonique des nappes et séries décollées de la partie centrale du versant sud des Pyrénées - Caractère synsedimentaire, rôle de la compresion et de la gravité. Publications USTELA, Montpellier, Série géologie structurale, 2, 155 p.

Sellés, J., 1988. Las correcciones estructural y tectónica en el tratamiento de los datos magnéticos. Geofísica Internacional, 27-3, 379-393.

Simó, A., 1985. Secuencias deposicionales del Cretácico superior de la Unidad del Montsec (Pirineo Central). Ph.D Thesis, Universidad de Barcelona, 326 p.

Soto, R., Casas, A.M., 2001. Geometría y cinemática de las estructuras norte-sur de la cuenca de Ainsa. Revista de la Sociedad Geológica de España 14, 3–4.

Soto, R., Casas, A.M., Storti, F. and Faccenna, C., 2002. Role of lateral thickness variations on the development of oblique structures at the western end of the South Pyrenean Central Unit. Tectonophysics 350, 215–235.

Soto, R.; Casas-Sainz, A.M.; Pueyo, E. L., 2006. Along-strike variation of orogenic wedges associated with vertical axis rotations. Journal of Geophysical Research (Solid Earth) 111, B10402 - B10423.

Stewart, S. A., 1995. Paleomagnetic analysis of plunging fold structures: Errors and a simple fold test, Earth Planetary Science Letters, 130: 57-67

Stewart, S. A.; Jackson, K. C., 1995. Palaeomagnetic analysis of fold closure growth and volumetrics. Geological Society Special Publications, vol.98, 283-295.

Sussman, A. J.; Pueyo, E. L.; Chase, C. G.; Mitra, G.; Weil, A. J., 2012. The impact of vertical-axis rotations on shortening estimates. Lithosphere, 4 (5), 383-394,

doi:10.1130/L177.1

Taberner, C., Dinarès-Turell, J., Giménez, J., Docherty, C., 1999. Basin infill architecture and evolution from magnetostratigraphic crossbasin correlations in the southeastern Pyrenean foreland basin, Geol. Soc. Am. Bull., 11, 1155 – 1174

Tavani, S., Storti, F., Fernández, O., Muñoz, J.A., Salvini, F., 2006. 3-D deformation pattern analysis and evolution of the Añisclo anticline, southern Pyrenees. Journal of Structural Geology 28, 695–712.

Tavani, S., Fernández, O., Muñoz, J. A. 2012. Stress fluctuation during thrust-related folding: Boltaña anticline (Pyrenees, Spain). Geological Society, London, Special Publications, 367(1), 131-140.

Tavani, S., López, B., Muñoz, J.A., 2015. Extensional fold-related fracturing in the Armeña rollover (Cotiella Massif, Southern Pyrenees). Ital. J. Geosci. http://dx. doi. org/10, 3301.

Teixell, A., 1996. The Ansó transect of the Southern Pyrenees: Basement and cover thrust geometries. J. Geol. Soc. London, 153:301-310.

Teixell, A., 1998. Crustal structure and orogenic material budget in the west central Pyrenees. Tectonics, 17 (3), 395-406.

Teixell, A., Muñoz, J.A., 2000. Evolución tectono-sedimentaria del Pirineo meridional durante el Terciario: una síntesis basada en la transversal del río Noguera Ribagorçana. Rev. Soc. Geol. España, 13, 2, 251-264.

Van der Voo, R., 1990. The reliability of paleomagnetic data. Tectonophysics, 184, 1-9.

Van der Pluijm, B.A., 1987. ‘Grain scale deformation and the fold test – Evaluation of

synfolding remagnetization', Geophys. Res. Lett. 14, 155–157.

Van Lunsen, H., 1970. Geology of the Ara-Cinca region, Spanish Pyrenees. Province of Huesca. Thesis, Utrech State University, 1970. Geol. Ultraiectina, 16: 1 -119.

Vergés, J., Muñoz, J.A., 1990. Thrust sequences in the Southern Central Pyrenees. Bull. Soc. Géol. Fr., 8, 6(2), 265-271.

Vidal-Royo, O., Cardozo, N., Muñoz, J.A., Hardy, S., Maerten, L., 2011. Multiple mechanisms driving detachment holding as deduced from 3D reconstruction and geomechanical restoration: The Pico del Águila anticline (External Sierras, Southern Pyrenees). Basin Research, 23, 1-19.

Vidal-Royo, O.; Muñoz, J.A.; Hardy, S.;Koyi, H.; Cardozo, N., 2013. Structural evolution of Pico del Águila anticline (External Sierras, southern Pyrenees) derived from sandbox, numerical and 3D structural modelling techniques. Geologica Acta 11 (1), 1 – 26.

Waldhör M. and Appel E., 2009. Layer parallelisation: An unrecognised mechanism for paleomagnetic rotations in fold belts. Tectonophysics 474, 516-525.

Weil, A. B., 2006. Kinematics of orocline tightening in the core of an arc; paleomagnetic analysis of the Ponga Unit, Cantabrian Arc, northern Spain. Tectonics, vol.25, no.3, 23

Zotkevich, I. A., 1972. Reduction of the natural remanent magnetization of a plunging fold to the ancient coordinate system in paleomagnetic studies. Earth Physics, 2: 95-99.

FIGURE CAPTIONS

Figure 1. (A) Geological sketch of the Southern Pyrenees. The Jaca Basin to the west and the Graus-Tremp Basin to the east of the Boltaña anticline can be distinguished. The study has been focused in the framed area. Modified from Oliva-Urcia et al. (2012). (B) Simplified structural units in the southwestern Pyrenees. (C) A-A': N-S cross section close to the Boltaña anticline. G: Gavarnie, Gu: Guarga, SE: External Sierras. Modified from Cámara and Klimowitz (1985). B-B': Geological cross-section between the Gavarnie tectonic window and the Guarga synclinorium, showing the main stratigraphic and tectonic units. The presented thickness (and dip) of units does not correspond exactly with actual thickness because of the obliquity of the cross-section with the strike of bedding.

Figure 2. A) Geological map of the studied area, modified from Barnolas et al. (*in press*). VAR sites are depicted as points. San Felices, Planillo and Arbella folds are shown. UTM Coordinate system, datum ED50, zone 30. B) Bingham (1974) fitting statistics of fold axes. Data from Boltaña come from Mochales et al. (2012b); Jánovas area axes come from compilation in this work, Barnolas et al. (*in press*) and Muñoz et al., 2013; Guarga axis from Barnolas et al. (*in press*).

Figure 3. Chronostratigraphic chart of the studied area.

Figure 4. Oblique photogeological sketch of the Jánovas fold system showing the main stratigraphic relationships between units. See text for explanation.

Figure 5. Geological 3D sketches of the evolution of the Jánovas area. Three main stages can be recognized. A) During the Early Lutetian, the Boltaña folding started related to Gavarnie thrust sheet emplacement. Folds involved show a variable Pyrenean trend between W-E and NW-SE. B) The main rotation of the Boltaña anticline occurred

in the Lutetian-Bartonian boundary and lasted till Middle Priabonian times. This rotation gradually modified from E to W the folds in the Jánovas area. C) In the Oligocene-Miocene interval the non-coaxial Guarga basement thrusting took place and tilted to the South the Jánovas previous structures according to a Pyrenean trend. The Boltaña thrust surface propagates and finally disappears within the Eocene, and does not crop out at the present-day erosion level.

Figure 6. Representative thermal demagnetization diagrams, stereoplots and intensity drops. NRM is 10^{-6} A/m magnitude. Data in diagrams are plotted *in situ* coordinates.

Figure 7. Magnetic mineralogy analysis. Lowrie test (1990) temperatures are represented in the x axis, and the normalized remanent magnetization in the y-axis. Four types of mineralogical content were defined. Types I and II (described in Mochales et al., 2012a) corresponds to magnetite-bearing and variable magnetite–iron sulfides-bearing rock types, respectively. Excepcionally, type IV presents an assorted magnetite–iron sulfide–hematite content.

Figure 8. Paleomagnetic stability. Equal area projection of data before and after the bedding correction. Three different situations were considered; the simple bedding correction (upper left) and after the removal of the tilting caused by the Guarga thrust. In this later case, two end-members were taken into account; 30° and 55° (lower part). The evolution of the concentration parameter during unfolding is also shown (upper right). Note that non of the tests are significant, although the k parameter is higher when the Guarga tilting was firstly removed, Note the improvement of the clustering observed in the inclination value after the restoration to the horizontal, a fact that supports the primary character of the magnetization.

Figure 9. Fold axes orientation at regional scale. The Basa anticline, Orosia syncline

and Guarga syncline fall within the expected Pyrenean trend (ESE-WNW), whereas the Boltaña and Balzes anticlines display the characteristic N-S trend of the Ainsa oblique zone. On contrary, the Jánovas area display interference patterns of folds where sequential restoration can be a useful tool to obtain reliable VARs.

Figure 10. Numerical comparisons in the stereonet (Allmendinger, 2012) of the fold axes in the studied region. A) Fold axes in their present-day orientation.The significant plunge of the studied folds (San Felizes, Planillo and Arbella) informs about their likely secondary origin of them. B) Restoration of fold axes after Guarga tilting, 30° and 55° of tilting were applied, the later removes completely the mean plunge of the folds axes while the smaller tilting returns a moderate (≈20°) plunge. This difference could support the higher angle of tilting against the moderate one. C) Complete restoration that evidences the abnormal fold axes orientation of the Jánovas superposed zone when compared to the Pyrenean expected trends.

Figure 11. Comparison of simple bedding and sequential correction in the different structural sectors considered. A) *In situ* (bac) Fisher (1953) means by W-E sectors with bedding field data. Overturned beds are shown with dashed lines. β: Vertical Axis Rotations (VAR). B) Simple restoration (abc) stages are presented. C) Sequential fold axis correction by W-E sectors; two end-members of tilting were considered; 120, 30 S and 120, 55 S. First step implies the removal of the Guarga tilting and the calculation of both, vectors and bedding planes (aGc+So'): the total (tectonic) restoration, is achieved when the remaining deformation is fully removed (bedding correction ; aTc). β: represents the vertical-axis rotation (Declination of the mean minus the declination of the reference).

Figure 12. Comparison of the deduced VARs after bedding correction and after the

sequential restorations carried out in a complex superposed folding area. Stereoplot of sector means in the three considered scenarios. Eocene reference (black star) is DEC: 004, INC: 55; α_{95}: 4° (Taberner et al., 1999). Mean rotation of the Boltaña-Ainsa hangingwall (Mochales et al., 2012b) is also projected for comparison (red star).

Table 1. Paleomagnetic data for individual sites arranged from E (San Felices syncline), central (Planillo anticline), to W (Arbella syncline) with Site: site label; n/N: number of specimens considered/measured; Pol: polarity; m: stratigraphic thickness of the site; Age and Age E: Age and Age error in M.y.; Chron; Formation; UTM coordinates in ED50, Zone 30; Strike, Dip, DD: bedding (rhr); o: overturned beds; Paleomagnetic *data in situ* (bac), after simple correction (abc), after Guarga correction (aGc), partial restoration of So (So-aGc), after total correction (aTc), error in the estimation of the VAR ΔaTc-abc. Rotations in each stage of restoration have been calculated (β) according to the Eocene reference (Taberner et al., 1999).

Table 2. Mean paleomagnetic data for the structural sectors considered. *In situ* (bac); after simple correction (abc); after Guarga correction (aGc); after total correction (aTc).

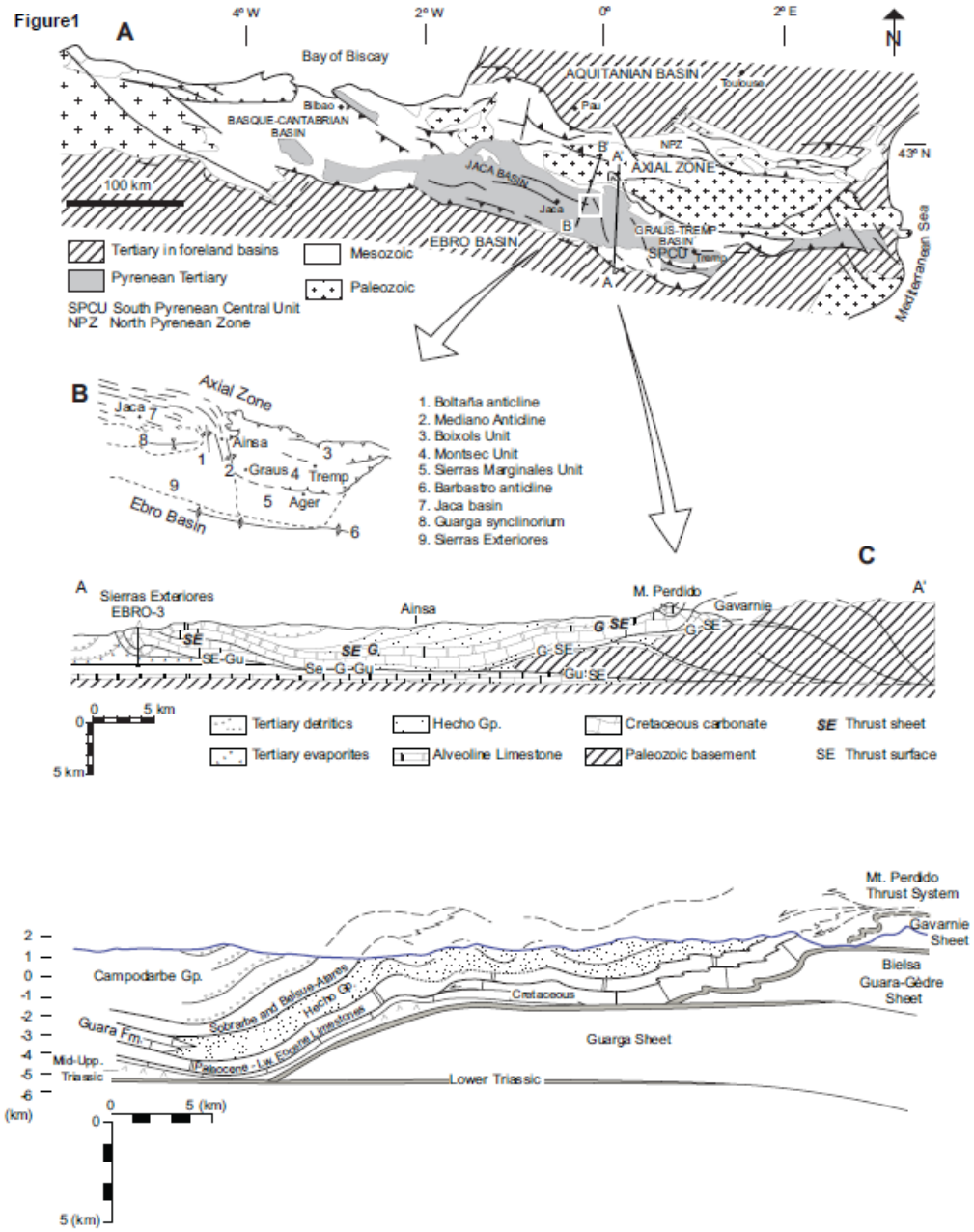

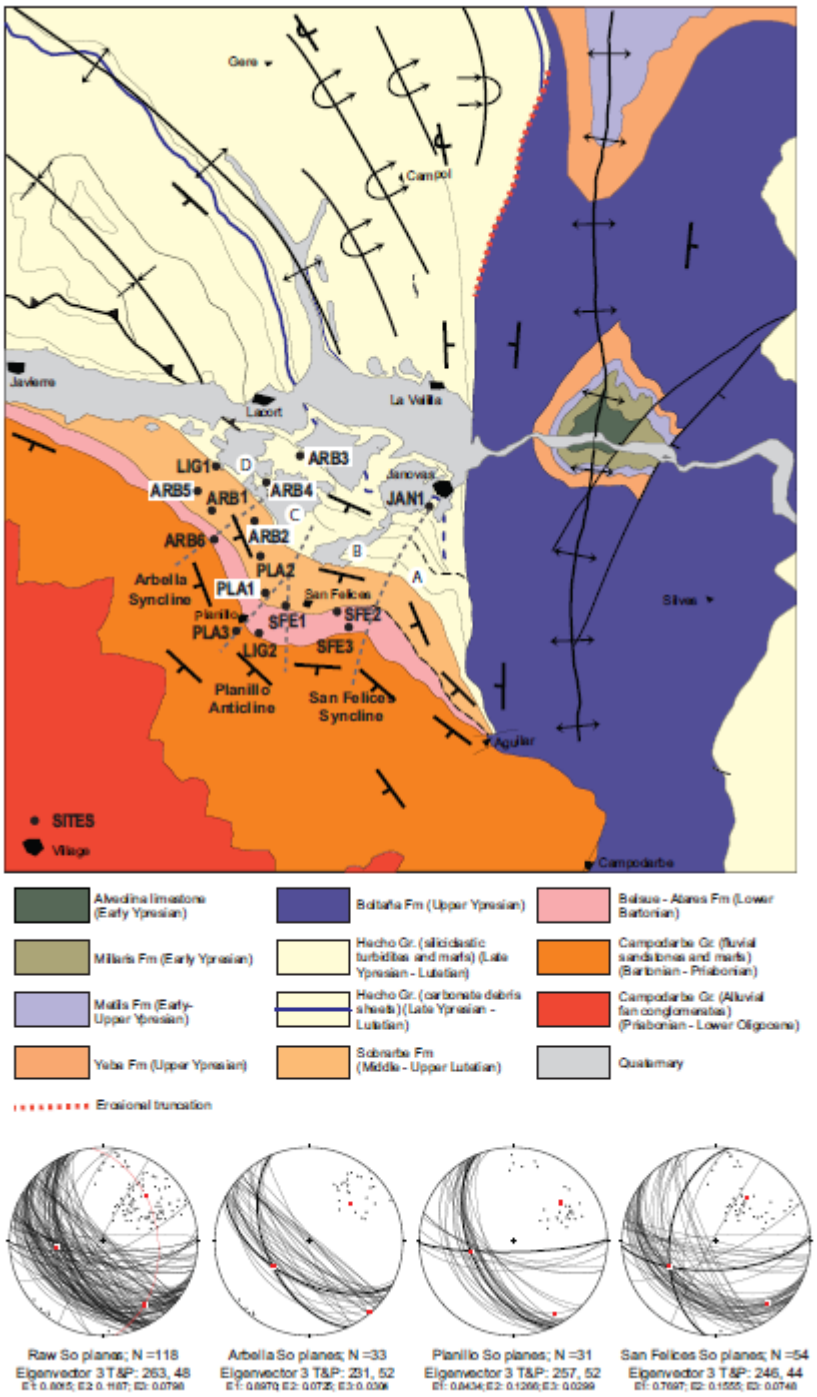

Figure 2

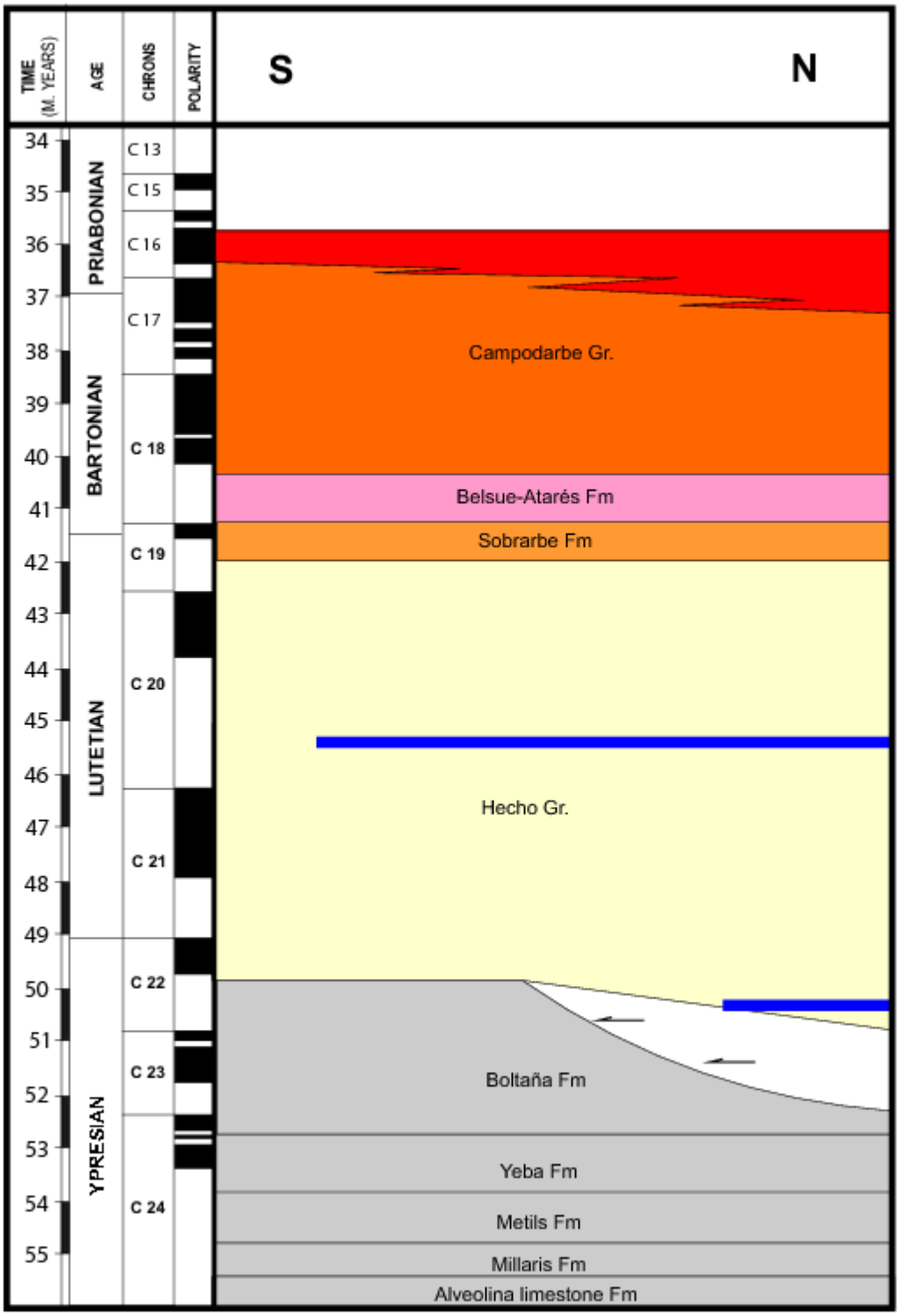

Figure 3

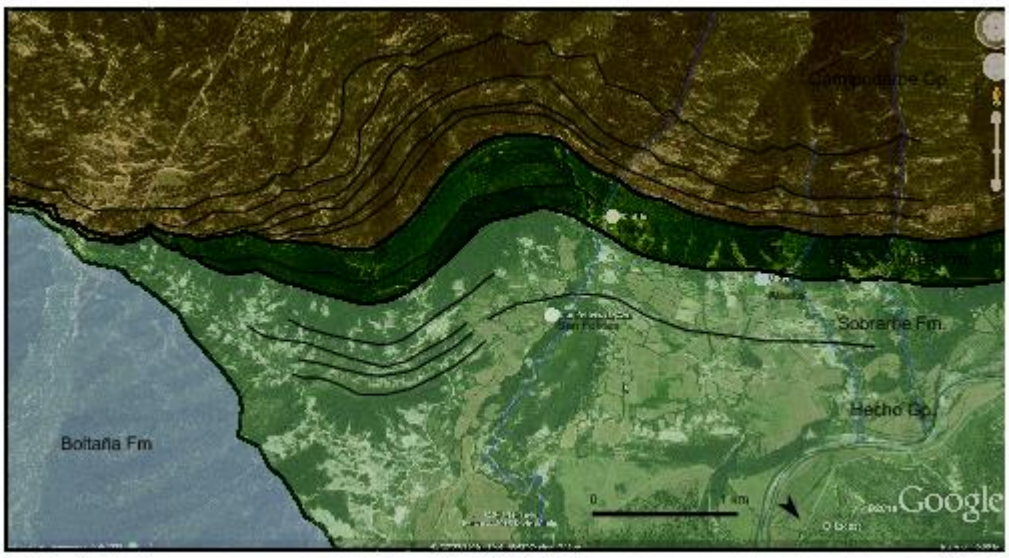

Figure 4

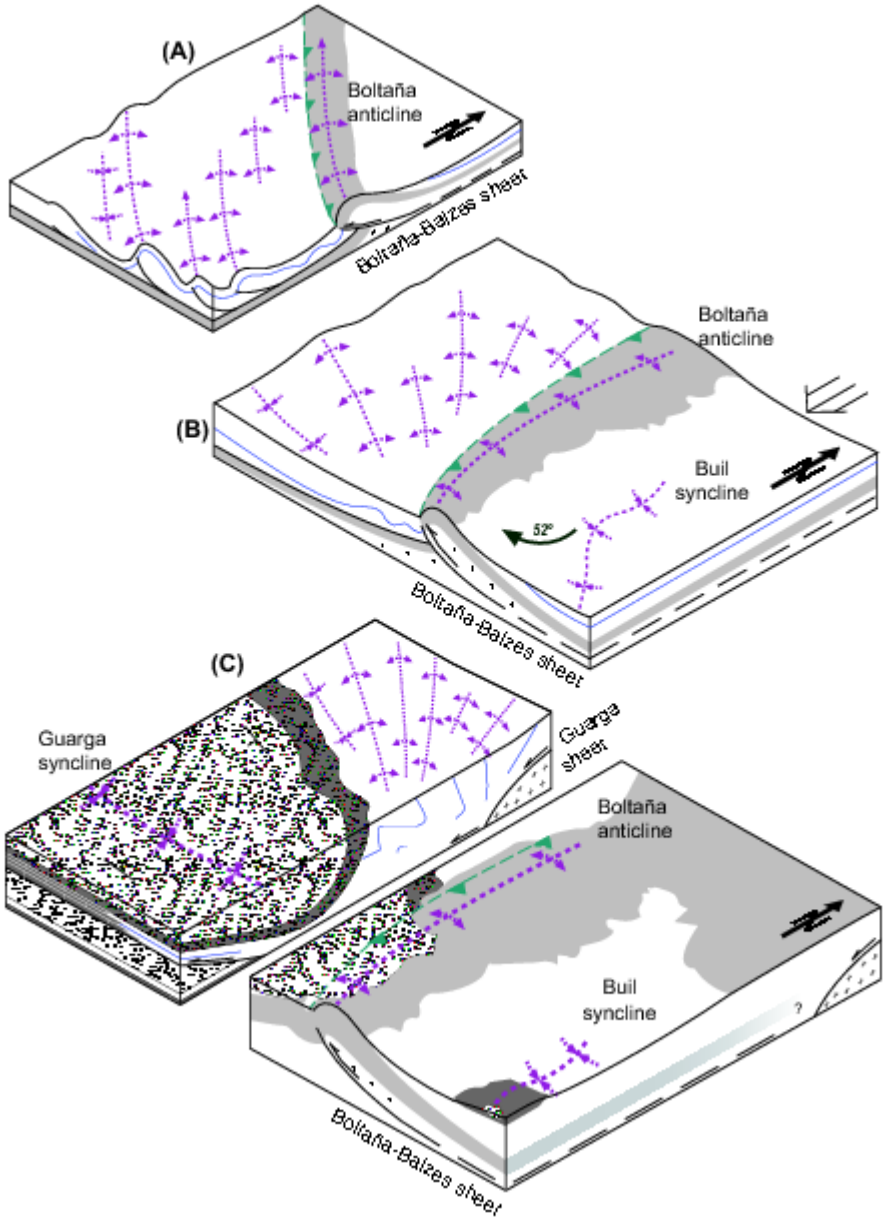

Figure 5

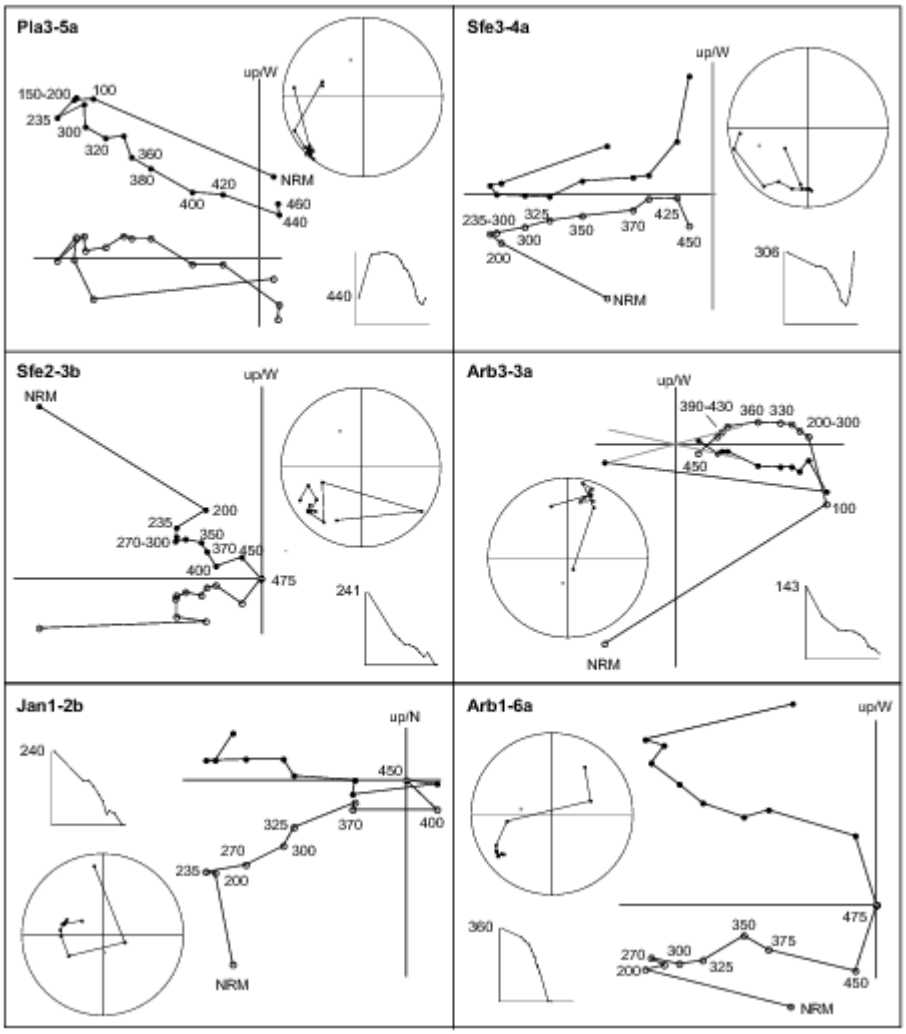

Figure 6

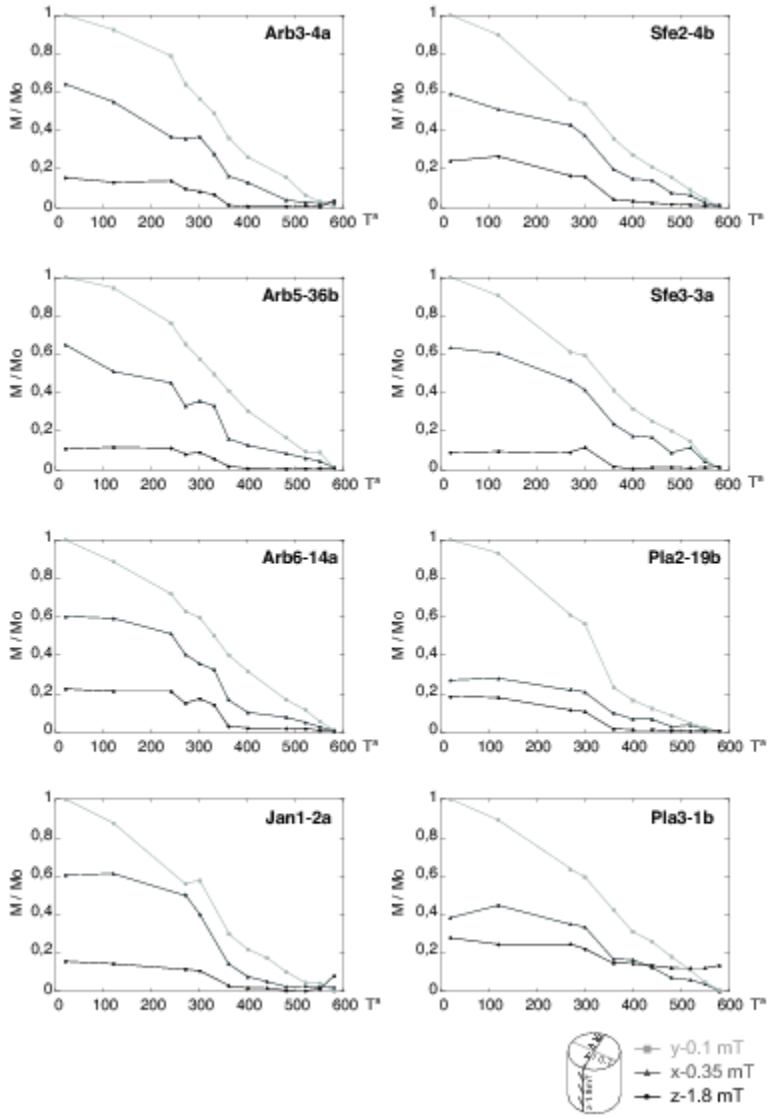

Figure 7

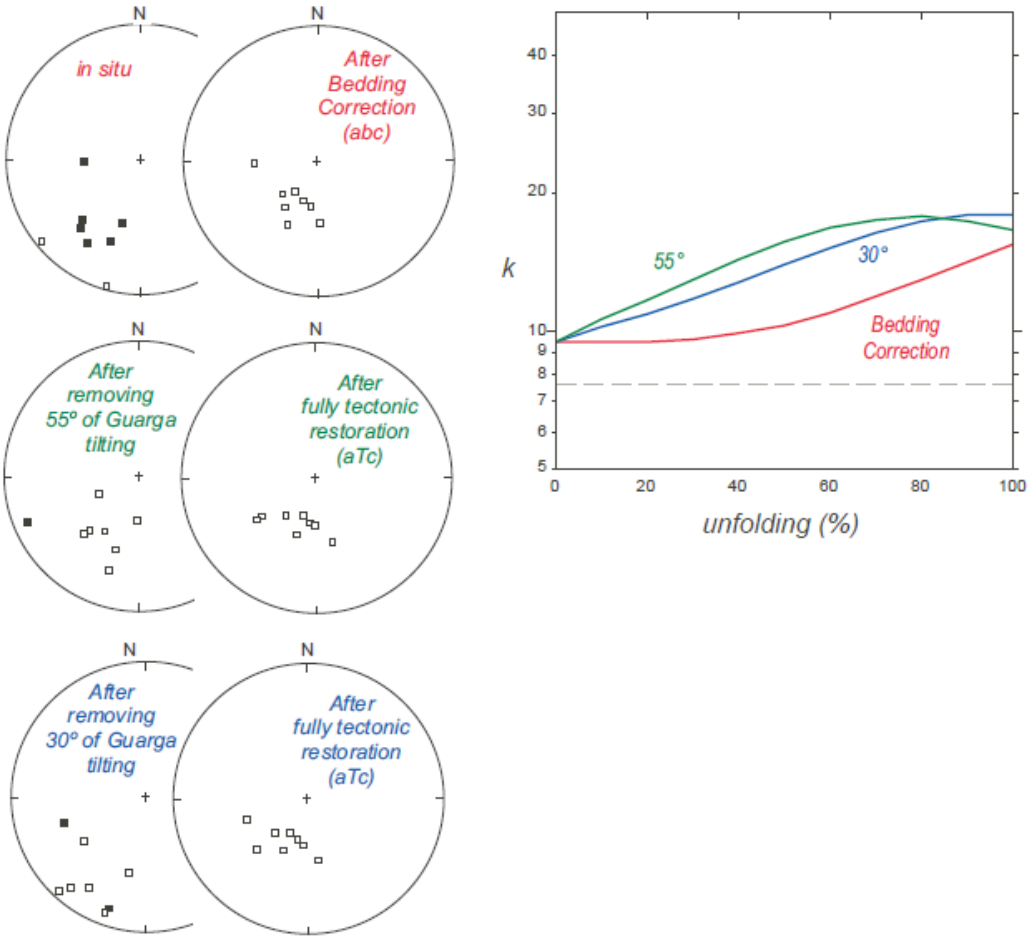

Figure 8

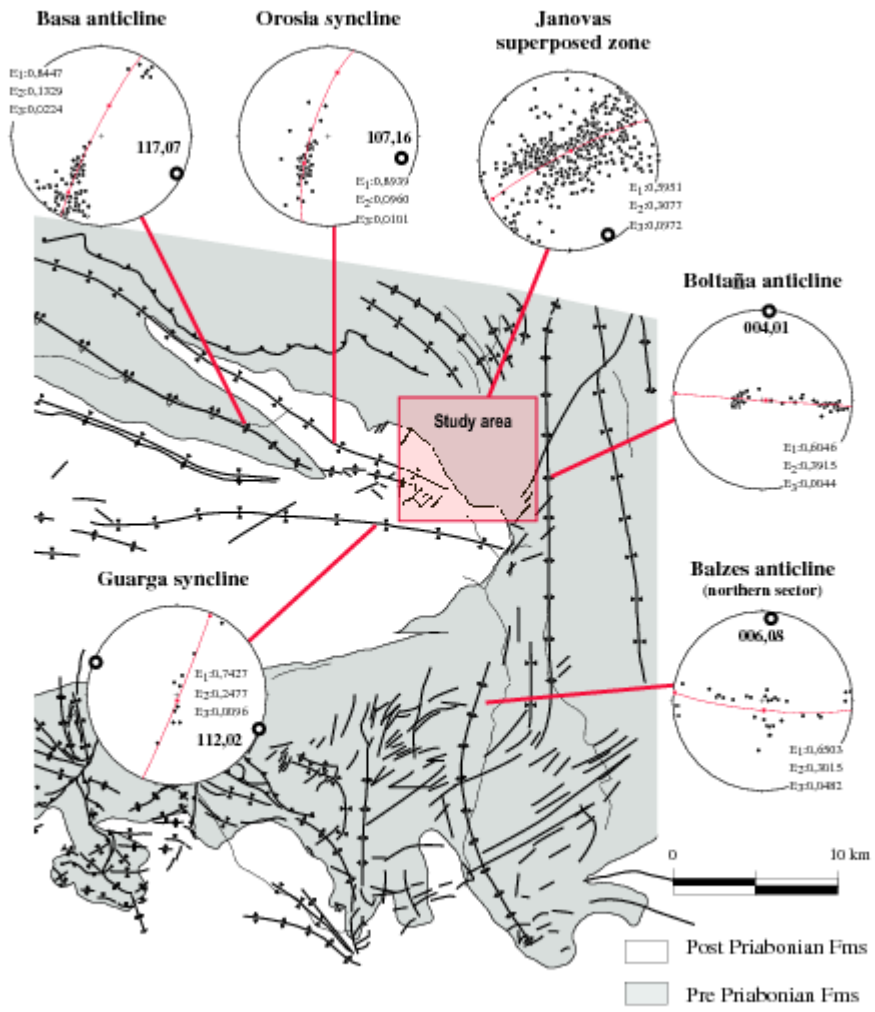

Figure 9

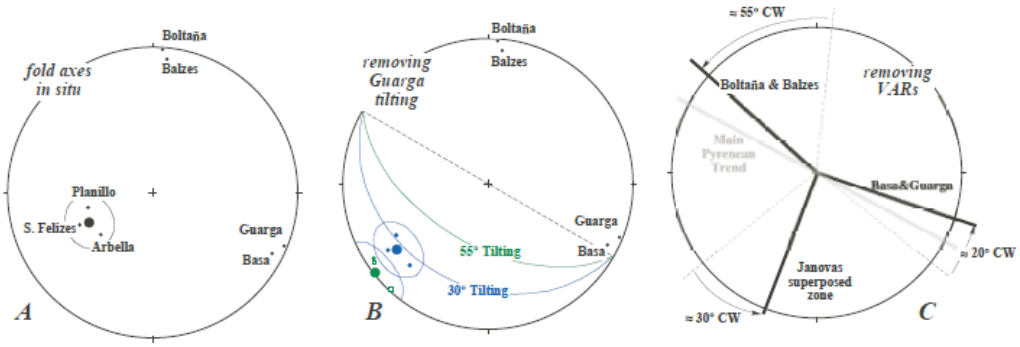

Figure 10

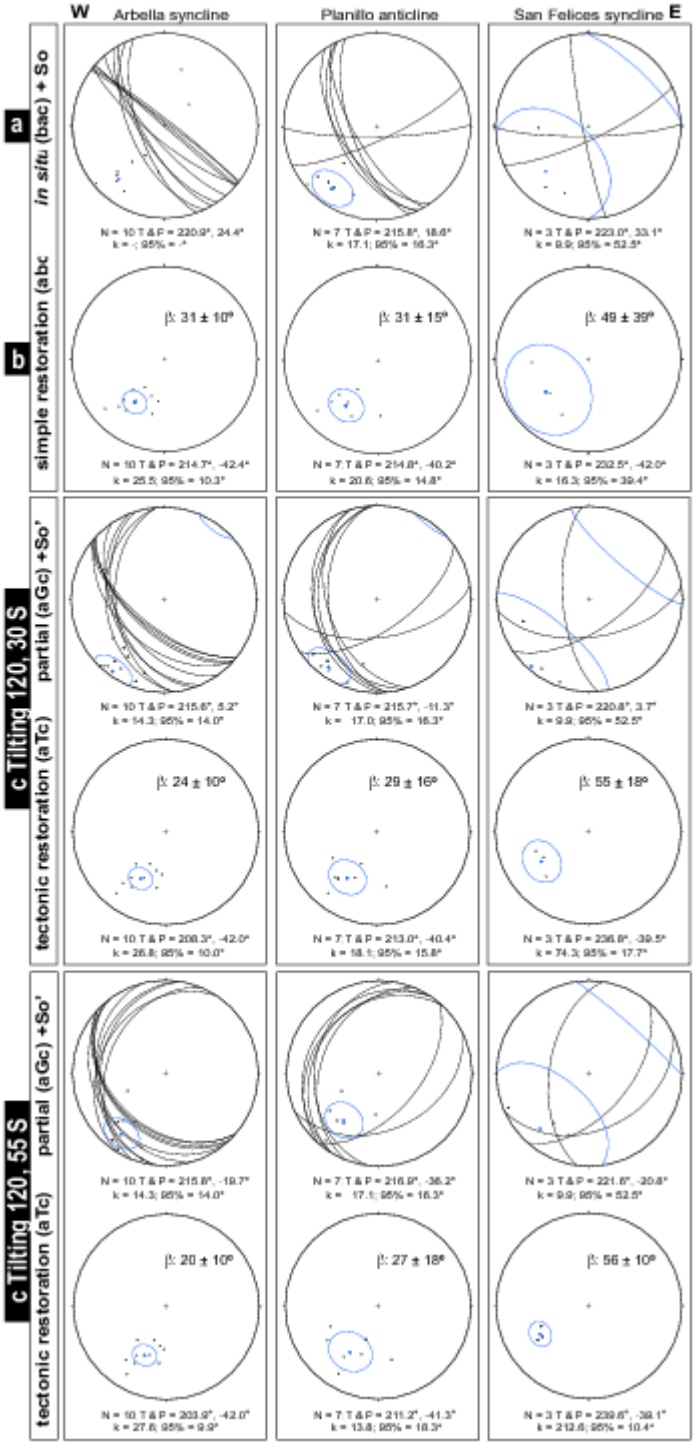

Figure 11

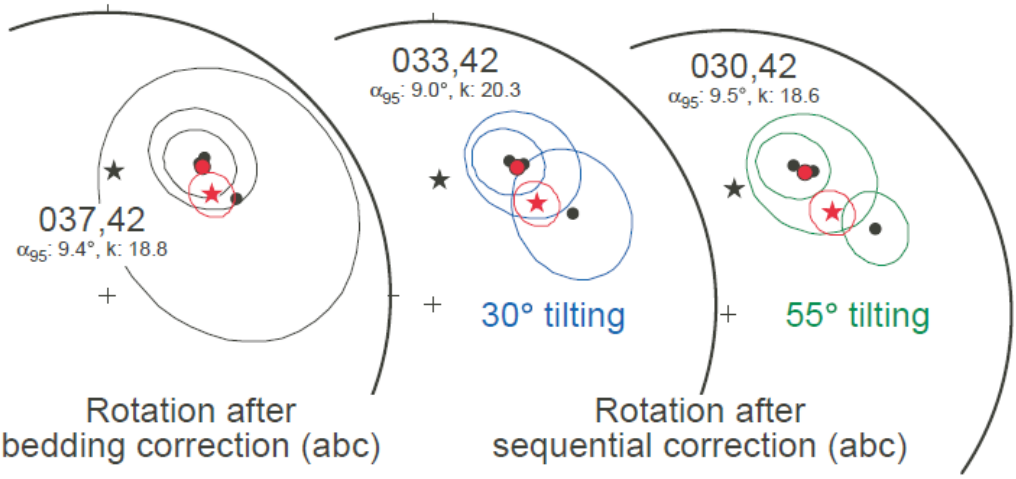

Figure 12

Table 1

			Site data (individual sites)							Field data (individual sites)						Paleomagnetic data (individual sites)									Strike 120 tilt 30°												Strike 120 tilt 55°										
Structure		Dip domain	Site	n/N	Pol	m	Age	Age E	Chron	Formation	UTM-X	UTM-Y	Strike	Dip	DD		D(bac)	I (bac)	a95(bac)	k(bac)	D(abc)	I (abc)	β (abc)		D(aGc)	I (aGc)	β (aGc)	Strike(aGc)	Dip(aGc)	DD(aGc)	D(aTc)	I (aTc)	β (abc)	ΔaTc-ABC				D(aGc)	I (aGc)	β (aGc)	Strike(aGc)	Dip(aGc)	DD(aGc)	D(aTc)	I (aTc)	β (abc)	ΔaTc-ABC	Δ55-30
	SAN FELIZES	A	JAN1	11/12	R	34	44.52	1.29	20r	Hecho Gp	746274	4705824	169	85	W		268	45	13.0	14.7	267	-39	87		252	25	68	175	66	W	249	-39	65	-18				247	6	63	188	54	W	237	-39	53	-31	-13
	SYNCLINE	B	SFE3	8/12	R	26	40.76	0.46	C19R	Belsué-Atarés Fm	745062	4703986	65	78	S		199	24	11.7	32.4	205	-34	25		200	-6	16	56	63	S	223	-34	39	18				198	-30	14	41	55	E	236	-34	52	31	13
	A+B	B	SFE2	10/12	R	30	41.14	0.46	C19R	Belsué-Atarés Fm	744923	4704196	89	81	S		215	21	15.5	11.8	228	-44	48		215	-9	31	82	56	S	240	-44	56	11				216	-34	32	65	38	S	247	-44	63	19	8
PLANILLO		B-C	SFE1	10/12	R	18	41.44	0.46	C19R	Sobrarbe Fm	744262	4704583	146	57	W		195	-1	12.3	18.3	177	-40	-3		193	-30	9	164	32	W	171	-40	-13	-6				184	-53	0	212	22	W	166	-40	-18	-11	-5
ANTICLINE		B-C	LIG2	10/10	R	5	42.27	0.58	C19r/19n	Belsué-Atarés Fm	743823	4704271	154	54	W		230	18	20.0	6.0	228	-34	48		229	-10	45	178	32	W	220	-34	36	-8				233	-34	49	222	28	W	214	-34	30	-14	-6
B+C		C	PLA1	5/12	N+R	16	40.99	0.46	C19R	Sobrarbe Fm	743997	4704750	160	67	W		222	46	28.3	10.3	230	-17	50		219	17	35	175	46	W	219	-17	35	-11				218	-8	34	202	37	W	210	-17	26	-20	-9
		C	PLA2	10/11	R	11	41.44	0.46	C19R	Sobrarbe Fm	743927	4705189	150	70	W		221	22	10.0	27.0	215	-44	35		220	-8	36	161	45	W	206	-44	22	-9				222	-32	38	188	30	W	199	-44	15	-16	-7
		C	PLA3	12/12	R	25	39.95	0.49	18R	Campodarbe Gp	743608	4704284	155	59	W		230	-3	7.6	37.0	215	-59	35		234	-31	50	175	37	W	206	-59	22	-9				245	-53	61	212	30	W	200	-59	16	-16	-7
		D	ARB3	9/13	R	18	42.52	0.59	C20N	Hecho Gp	744478	4706401	128	95	S	o	16	-37	9.9	37.1	9	52	9		19	-8	15	129	65	S	5	52	1	-4				18	17	14	132	41	S	3	52.2	-1	-6	-2
	ARBELLA	D	ARB2	8/12	N+R	20	41.67	0.59	C20N	Sobrarbe Fm	743858	4705605	130	91	S	o	48	-62	28.1	6.5	44	29	44		40	-33	36	131	62	S	40	29	36	-4				38	-8	34	137	37	W	37	29	33	-7	-3
	SYNCLINE	D	ARB4	6/12	N+R	20	42.10	0.59	C20N	Hecho Gp	743999	4706054	131	89	S		214	58	33.3	6.0	217	-31	37		212	28	28	133	60	S	212	-31	28	-5				212	3	28	139	36	W	209	-31	25	-7	-3
	C+D	D	ARB6	12/13	R	10	40.84	0.46	C19R	Belsué-Atarés Fm	743289	4705323	139	76	W		212	17	11.7	16.1	200	-55	20		212	-13	28	145	48	W	194	-55	10	-7				212	-38	28	164	27	W	189	-55	5	-11	-4
		D	ARB1	10/12	R	22	41.29	0.46	C19R	Sobrarbe Fm	743279	4705764	129	77	S		224	26	7.1	52.3	226	-51	46		223	-3	39	132	48	S	223	-51	39	-3				224	-28	40	143	24	W	221	-51	37	-5	-2
		D	LIG1	10/10	R+N		40.67	0.59	C20N	Sobrarbe Fm	743317	4706473	146	68	W		226	29	22.0	5.0	225	-38	45		224	0	40	157	42	W	217	-38	33	-8				225	-24	41	187	26	W	212	-38	28	-13	-6
		D	ARB5	9/12	N+R	12	41.58	1.05	C20N/19R	Sobrarbe Fm	743197	4705981	127	93	S	o	188	48	27.8	4.4	193	-39	13		195	20	11	128	63	S	189	-39	5	-3				195	-5	11	131	39	S	188	-39	4	-5	-2

Table 2

	Simple bedding correction								Strike 120 tilt 30°								Strike 120 tilt 55°							
E-W Sector	bac				abc				aGc				aTc				aGc				aTc			
	Dec	Inc	a95	k	Dec	Inc	a95	k	Dec	Inc	a95	k	Dec	Inc	a95	k	Dec	Inc	a95	k	Dec	Inc	a95	k
San Felices syncline (E)	223	33	52.5	9.9	53	42	39.4	16.3	41	-4	52.5	9.9	57	40	17.7	74.3	222	-21	52.5	9.9	60	39	###	####
Planillo anticline (Central)	216	19	16.3	###	35	40	14.8	20.6	36	11	16.3	17.0	33	40	15.8	18.1	217	-36	16.3	17.1	31	41	###	13.8
Arbella syncline (W)	221	24	-	-	35	42	10.3	25.5	33	-5	14.5	13.3	28	42	10.0	26.8	216	-20	14.0	14.3	24	42	9.9	27.6
	217	19	18.1	5.8	37	42	9.4	18.8	36	-1	12.2	11.5	33	42	9.0	20.3	217	-24	12.2	11.5	30	42	9.5	18.6

Highlights

Highlights

Sequential restoration follows the reverse order of the deformation events

Structural analysis must justify the parameters applied to the sequential restoration

Paleomagnetic data in complex scenarios is restored by sequential restoration

A case study of non-coaxial folding in Pyrenees helps highlighting its importance

Simple bedding correction may produce up to 30° of apparent rotations in some sites